M 2018

U.PORTO
FEUP FACULDADE DE ENGENHARIA
UNIVERSIDADE DO PORTO

HYDROGEN GENERATION FROM SODIUM BOROHYDRIDE

THE EFFECT OF NI-RU SUPPORTED CATALYST IN THE HYDROLYSIS REACTION

EMÍLIA ISABEL DE CASTRO E CÂMARA FREITAS VALADÃO

DISSERTAÇÃO DE MESTRADO APRESENTADA
À FACULDADE DE ENGENHARIA DA UNIVERSIDADE DO PORTO EM 16 DE FEVEREIRO DE 2018
ENGENHARIA QUÍMICA

Master in Chemical Engineering

Hydrogen generation from Sodium Borohydride – The effect of Ni-Ru supported catalyst in the hydrolysis reaction

A Master's dissertation

of

Emília Isabel de Castro e Câmara Freitas Valadão

Developed within the course of Dissertation

held in

CEFT – Centro de Estudos de Fenómenos de Transporte

Faculdade de Engenharia da Universidade do Porto

Supervisor: **Prof. Dr. Alexandra Rodrigues Pinto (CEFT – DEQ)**

Chemical Engineering Department

February of 2018

To my dad Paulo,

Someone who always wanted to learn more

And passed away too soon

While he was learning about hydrogen generation.

Acknowledgments

This work wouldn't be possible without some important people which are referred below.

To my supervisor, Dr. Alexandra Pinto, for the opportunity to let me do my thesis in a study area that I really enjoy and for all the guidance.

To Helder Nunes, who co-supervised and helped me every time I needed during the past six months. I also want to thank him for letting me work freely, teaching me much more about hydrogen generation, for providing the visit to CEMUP and finally for his amazing support when I called telling him that I needed to go to Flores in an emergency.

To all the CEFT members that welcomed me so well and for the comfortable environment that they provided namely to Diogo that helped me in the first days at CEFT.

To *Laboratório Nacional de Energia e Geologia* (LNEG) and particularly to Dr. Cármen Rangel for synthesizing the catalysts used in all this work.

To Daniela Silva for all the explanations about the SEM analysis in *Centro de Materiais da Universidade do Porto* (CEMUP).

To my colleagues from university that somehow helped me during these months and the whole course and for their friendship, in special to my colleagues working at DEQ, for their fellowship and for the snacks at Friday.

To my best friends from Flores for all tireless support, for being present even though they are far away and for the good times.

To my cat that even without knowing helped me to maintain my mental sanity, I couldn't finish my thesis without thanking him.

To Nuno, that helped me since the beginning of this thesis, for his love and infinite support and for bearing me when I talked about hydrogen. I also want to thank to his family for the amiability and for the companionship they offered me all the time.

And in special to my family. To my little nephews from the heart, Mitó for remembering me that the world can be so pinky and Joãozico for teaching me that love can be so innocent and for asking me if I could stay with him in Flores to play. To my cousin Luisa, for being the sister that I didn't have and for helping me in the English revision of my thesis. To my grandmother Maria José, for always being present in my life, for the motivation and for the prays since the beginning of my course. And most of all, to my parents, Dora and Paulo, the pillars of my life, for all the economic support and for being present, thank you for not letting me quit anything.

I want to dedicate my thesis in loving memory of my dad Paulo, that was supposed to be present in the defense of my thesis and I am sure that he would be so proud.

Abstract

Climate change is becoming more remarkable each day and it is the biggest environmental threat of the 21st century. This is in part caused by the excessive use of fossil fuels and, consequently, by the increase levels of air pollution. Therefore, it is necessary to reduce the use of these fuels and replace them by "clean" energy sources, i.e., sources that do not release pollutants into the atmosphere while producing energy. Although hydrogen cannot be seen as an energy source, since it rarely exists in nature in its elemental state, it can be seen as an energy carrier. Hydrogen can be stored through chemical hydrides, such as sodium borohydride, addressing the problem of hydrogen storage (liquefied or compressed). The hydrolysis reaction of sodium borohydride is safe, since it occurs at moderate pressure and temperature, and the generated hydrogen can be directly fed to a proton exchange membrane fuel cell (PEM), which can be widely used on a large range of applications, mainly portable devices.

The performance of two types of Ni-Ru catalysts supported and unsupported in the sodium borohydride hydrolysis was studied (the supported was tested for the first time within the research group), as well as, the influence of the following parameters: hydration factor, temperature (only for the unsupported catalyst), catalyst/$NaBH_4$ mass ratio and sodium borohydride amount (both only for the supported catalysts). The classic hydrolysis and alkali-free hydrolysis experiments were carried out in an ovoid mini-reactor. Furthermore, the catalysts were analysed through scanning electron microscopy (SEM), energy dispersive X-ray spectroscopy (EDX) and by X-ray diffraction (XRD).

From the results obtained, the hydrogen generation rate of 5 775 $mL_{H_2} min^{-1} g_{Cat}^{-1}$, achieved using the unsupported catalyst, at 50 ± 5 ºC and with a hydration factor of 11 stands out. Nevertheless, the use of a higher temperature is not suitable, since the yield obtained was low and it requires to spend energy – is intended to generate energy without using any external energy source. Regarding the supported catalysts results, a hydrogen generation rate of 5 463 $mL_{H_2} min^{-1} g_{Cat}^{-1}$ was obtained, at uncontrolled room temperature, with a hydration factor of 16 and a nickel foam with 0.44 mg of catalyst. The use of this type of catalysts is advantageous mainly due to its easier handling and cleaning processes. Furthermore, with these innovative catalysts, high hydrogen generation rates were achieved, at uncontrolled room temperature, that compete directly with the rates obtained at high temperature. This is a strong advantage bearing in mind portable applications. Nevertheless, all the supported catalysts showed a quick degradation.

Keywords: Hydrogen generation; Sodium borohydride hydrolysis; Ni-Ru catalyst; unsupported catalysts; supported catalysts.

Resumo

As alterações climáticas são cada vez mais notáveis e são a maior ameaça ambiental do século XXI. Estas são, em parte, causadas pela utilização desmedida de combustíveis fósseis e consequentemente pelo aumento dos níveis de poluição atmosférica. Por isso, é necessário reduzir o uso destes combustíveis e substituí-los por fontes de energia "limpa", i.e., que não libertam poluentes para a atmosfera enquanto produzem energia. O hidrogénio não pode ser visto como uma fonte de energia, uma vez que não se encontra disponível no seu estado elementar, contudo deve ser visto como um potencial vetor energético. O hidrogénio pode ser armazenado através de hidretos químicos, como o borohidreto de sódio, colmatando a barreira do armazenamento do hidrogénio (liquidificado ou comprimido). A reação de hidrólise do borohidreto de sódio é segura, uma vez que ocorre a pressão e temperatura moderadas e o hidrogénio produzido pode ser diretamente alimentado a uma célula de combustível de eletrólito de membrana polimérica (PEM), fornecendo energia a uma vasta gama de aplicações.

Foram realizados estudos da hidrólise clássica e *alkali-free* do borohidreto de sódio para estudar o desempenho de dois tipos de catalisadores de Ni-Ru suportados (testados pela primeira vez no grupo de investigação) e não suportados. Foi avaliada a influência dos seguintes parâmetros: fator de hidratação, temperatura (apenas nos testes com o catalisador não suportado), a relação de massa catalisador/$NaBH_4$ e a quantidade de borohidreto de sódio (ambos apenas nos testes com os catalisadores suportados). As experiências foram realizadas num mini reator ovoide. Os catalisadores foram caracterizados por microscopia eletrónica de varrimento (SEM), por espetroscopia de raios X por energia dispersiva (EDX) e por difração de raios X (XRD).

A maior taxa de geração de hidrogénio alcançada neste trabalho foi de 5 775 $mL_{H_2} min^{-1} g_{Cat}^{-1}$, obtida com o catalisador não suportado, a 50 ± 5 ºC e com um fator de hidratação de 11. Contudo, tendo em conta que se pretende criar uma tecnologia de produção de energia sem utilizar uma fonte de energia externa, a utilização de uma temperatura mais elevada não é rentável. Relativamente aos resultados obtidos com os catalisadores suportados, uma taxa de produção de hidrogénio de 5 463 $mL_{H_2} min^{-1} g_{Cat}^{-1}$ foi alcançada utilizando uma espuma de níquel com 0.44 mg de catalisador, numa experiência realizada à temperatura ambiente, com um fator de hidratação de 16. Foi observado que este tipo de catalisador facilita o manuseamento e o processo de limpeza quer do próprio catalisador quer do reator. Foram obtidas taxas de produção de hidrogénio que competem diretamente com os valores obtidos a elevadas temperaturas, o que representa uma vantagem para aplicações portáteis. No entanto, todos os catalisadores suportados apresentaram uma rápida degradação.

Palavras Chave: produção de hidrogénio; hidrólise do borohidreto de sódio; catalisador de Ni-Ru; catalisadores não suportados; catalisadores suportados.

Declaration

I hereby declare, on my word of honour, that this work is original and that all non-original contributions were properly referenced with source identification.

Porto, 5th February 2018

Emília Isabel Valadão

(Emília Isabel de Castro e Câmara Freitas Valadão)

Index

Index of figures

Index of tables

Notation and Glossary

dP/dt	Linear region slope	bar s^{-1}
E_A	Activation energy	kJ mol^{-1}
GHSC	Gravimetric Hydrogen Storage Capacity	wt%
HGR	Hydrogen Generation Rate	mL_{H_2} min^{-1} g^{-1}_{Cat}
m_{Cat}	Catalyst mass	g
$m_{H_{2_{Exp}}}$	Mass of hydrogen obtained experimentally	g
m_{H_2O}	Mass of water	g
m_{NaBH_4}	Mass of sodium borohydride	g
m_{sol}	Mass of the solution	g
MM_{H_2O}	Molar mass of water	g mol^{-1}
MM_{NaBH_4}	Molar mass of sodium borohydride	g mol^{-1}
$P_{Gas_{Exp}}$	Absolute pressure of the gas produced	bar
$P_{Gas_{Theo}}$	Theoretical absolute pressure of the gas	bar
R	Ideal gas constant	cm^3 bar K^{-1} mol^{-1}
T	Temperature	K
T_{in}	Temperature inside the reactor	ºC
T_{out}	Temperature outside the reactor	ºC
V_{cat}	Volume of catalyst	cm^3
V_{final}	Final volume of the reactor	cm^3
V_{H_2O}	Volume of water	cm^3
VHSC	Volumetric Hydrogen Storage Capacity	kg m^3
V_{inital}	Initial volume of the reactor	cm^3
V_{NaBH_4}	Volume of sodium borohydride	cm^3
V_R	Total volume of the reactor	cm^3
V_{sol}	Volume of the reactant solution	cm^3
V_{STP}	Molar volume at STP conditions	22.466 L mol^{-1}
x	Hydration factor	

Greek letters

$\Delta H^0_{f,298K}$	Standard enthalpy of formation of a compound at 298 K	kJ mol^{-1}
$\Delta H_{products}$	Enthalpy of the products	kJ

$\Delta H_{reaction}$	Enthalpy of reaction	kJ
$\Delta H_{reactants}$	Enthalpy of the reactants	kJ
η	Yield rate	%
ρ_{Cat}	Volumetric mass density of the catalyst	g cm^{-3}
ρ_{H_2O}	Volumetric mass density of water	g cm^{-3}
ρ_{sol}	Volumetric mass density of the solution	g cm^{-3}

List of Acronyms

AFC	Alkaline Fuel Cell
BSE	Backscattered Electrons
CEMUP	*Centro de Materiais da Universidade do Porto*
DMFC	Direct Methanol Fuel Cell
DOE	Department of Energy
EDX	Energy Dispersive X-Ray Spectroscopy
LCA	*Laboratório Central de Análises*
LNEG	*Laboratório Nacional de Energia e Geologia*
MCFC	Molten Carbonate Fuel Cell
MEA	Membrane Electrode Assembly
PAFC	Phosphoric Acid Fuel Cell
PEMFC	Proton Exchange Membrane Fuel Cell
SE	Secondary Electrons
SEM	Scanning Electron Microscopy
SOFC	Solid Oxide Fuel Cell
STP	Standard Temperature and Pressure
U.S.	United States
XRD	X-Ray Diffraction

1. Introduction

"I believe that water will one day be employed as fuel, that hydrogen and oxygen which constitute it, used singly or together, will furnish an inexhaustible source of heat and light, of an intensity of which coal is not capable." Jules Verne[1] in The Mysterious Island

1.1 Motivation

Climate change is a worldwide problem which becomes more visible every day. Due to the exponential increase of population, it is expected that the demand for energy increases drastically and since the fossil fuels, as coal or oil, are the most used energy sources and their supply is limited, this increase will be a concern to the population. It is known that fossil fuels have an important role in atmospheric pollution, so there has been an effort to develop renewable and clean sources of energy [1].

Hydrogen is the most abundant element in the world and its properties, such as lightness and a higher calorific value, contribute to a vision of a hydrogen economy, where hydrogen will be the main energy carrier [2]. Table 1 shows the calorific values for different types of fuels, where hydrogen stands out as a fuel with more energy per unit of weight, i.e., it presents higher values both of high and low calorific values.

Table 1 – Calorific values for different types of fuels [3].

Fuel	High Calorific Value at 25°C and 1 atm (kJ g^{-1})	Low Calorific Value at 25°C and 1 atm (kJ g^{-1})
Hydrogen	141.86	119.93
Methane	55.53	50.02
Propane	50.36	45.60
Gasoline	47.50	44.50
Diesel	44.80	42.50
Methanol	19.96	18.05

The biggest disadvantage to hydrogen economy is the hydrogen storage since this element has a low volumetric energy density. Thus, it is necessary to discover a way to store hydrogen in a safe and economic viable mode. A possible technology to store hydrogen is through chemical hydrides, due to their high gravimetrical and volumetric hydrogen storage capacities, which offer great potential. Sodium borohydride ($NaBH_4$) is one of the chemical hydrides with higher hydrogen content, 10.8 wt%, which is suitable for portable applications; however, for on-board

[1] French poet (February 1828 – March 1905)

vehicular storage, the U.S. Department of Energy (DOE) has recommended a no-go for this type of storage with aqueous solution of $NaBH_4$. One of the main reasons for this decision was due to the low gravimetric and volumetric storage capacities obtained, that did not reach the targets [4], [5].

From a theoretical point of view, the hydrolysis reaction of sodium borohydride generates hydrogen according to Equation 1.1, nevertheless, in real conditions, the reaction needs an excess of water which will be explained in the next chapter [5]. It is an exothermic reaction and at 25 ºC has a standard state enthalpy change of -216.8 kJ, as it was calculated in Appendix A [4].

$$NaBH_4 + 2\,H_2O \rightarrow NaBO_2 + 4\,H_2 + \text{heat} \qquad (1.1)$$

On a weight basis, this reaction is extremely efficient, since it only has one by-product and it produces 4 moles of hydrogen, half from which comes from water and the other half from the $NaBH_4$, allowing us to state that the fuel - $NaBH_4$ solution - is acting as a hydrogen carrier and storage medium [6].

The hydrolysis of $NaBH_4$ is spontaneous, which means that when the reactants are used as a solution an additional element, such as sodium hydroxide, is needed to slow-down the reaction process. Therefore, it is necessary a catalyst to speed-up the reaction and consequently decrease the activation energy and increase the hydrogen generation rate [5]. Schlesinger *et al.* [7] recognized that some transition metals and their salts had a remarkable effect on the hydrolysis rate and in fact the metallic catalysts are often used, since the catalyst transfers electrons to the molecular water to generate hydrogen [8]. One of the biggest issues of this technology is the deterioration of the catalyst, for instance, due to the agglomeration of catalyst particles, surface oxidation of catalyst and dissolution of a catalyst component in $NaBH_4$ solutions [1].

A great advantage of generating hydrogen catalytically from $NaBH_4$ stabilized solutions is the fact that the reaction only occurs in the presence of selected catalysts, and, consequently, the generation rates of H_2 can be easily controlled and can occur even at 0 ºC. Moreover, the solutions of $NaBH_4$ are non-flammable and stable in air, the reaction products are environmentally safe, and the gas stream is composed only by water (besides the main product). There is also the possibility of recycling the by-product, $NaBO_2$, however this process is difficult and expensive [6].

The most prominent application of the hydrogen from $NaBH_4$ is to supply a proton exchange membrane fuel cell (PEMFC), which will power portable electronic devices, such as mobile phones, and have a major impact especially for remote locations. This fuel cell can also be used in vehicles (and it can equally be suitable for marine vehicles since hydrogen can be

obtained from water). Currently the cost of $NaBH_4$ production is too high to use in civil applications. Nevertheless, it is considered that if a way to easily recycle the by-product will be implemented, the cost of production would decrease [8].

1.2 Objectives

The main goal of this work is the study of the effect of two different Ni-Ru catalysts, in the rate and yield of the hydrolysis reaction of sodium borohydride to generate hydrogen, at moderate pressure and room temperature, using a mini reactor with an ovoid geometry. It is also important to learn about the hydrolysis reaction of sodium borohydride, both in alkali and alkali-free conditions as well as its advantages and disadvantages to use in portable applications.

Thus, several experiments were carried out using two types of catalysts: an unsupported catalyst of nickel and ruthenium in a powder form, and a ruthenium catalyst supported on a nickel foam (used for the first time within the research group). Three different foams, with different ruthenium concentrations were used to study the performance of the catalysts and compare to others described in the literature. It was also taken in account the operation conditions, such as the hydration factor and the temperature, in order to improve the rates of the reaction.

Furthermore, this research is done in the prospect of obtaining qualitative results for the research of an efficient catalyst, improving the vision of $NaBH_4$ as a hydrogen carrier and to corroborate the viability of its employment in portable applications.

1.3 Organization of the thesis

The current work is divided in seven main chapters.

Chapter 1, **Introduction**, where there is a first approach to the research theme and the presentation of the main objectives as well as the organization of the thesis.

Chapter 2, **Context and State of the Art**, contains a historical perspective of the hydrolysis of sodium borohydride and highlights more facts about hydrogen as an energy carrier and chemical hydrides, namely sodium borohydride. It also presents an overview of catalysts for sodium borohydride hydrolysis, reporting some of the most significant results for noble metal catalysts and a small description of the reactors most commonly used for this reaction. Finally, there is a summary about fuel cells, emphasizing the proton exchange membrane fuel cells and its operation principle.

Chapter 3, **Materials and Methods**, describes the materials used in this work and also explains the experimental setup and procedure.

Chapter 4, **Results and Discussions**, is focused on the results obtained in the several experiments which are analysed and compared with the values referred in the literature.

Chapter 5, **Conclusions**, discusses the main conclusions of this thesis.

Chapter 6, **Assessment of the work done**, refers to the difficulties faced during the development of this work and some suggestions for future research.

Finally, there is the bibliography used in this thesis in Chapter 7, **References**.

2. Context and State of the art

This chapter introduces a brief history about the discovery of hydrogen production from the hydrolysis of sodium borohydride and the potential use of hydrogen as an energy carrier, highlighting the concept of hydrogen economy. The characteristics of sodium borohydride as a chemical hydride are also described, as well as a review of nickel-ruthenium based catalyst, including a literature overview of noble metal catalysts. To conclude this chapter, the different types of reactors used in sodium borohydride hydrolysis are presented, and it is made a small approach to the main application of hydrogen in fuel cells and its operating mode.

2.1 Brief history

Schlesinger and the winner of the Nobel Prize in Chemistry in 1979, Herbert Brown, [7] were the first authors to report the generation of hydrogen by hydrolysis of $NaBH_4$ in early 1950's although only in the late 1990's the research in the field grew significantly.

In 1962, Brown and Brown [9] investigated a series of metal salts and concluded that ruthenium and rhodium salts liberated hydrogen most quickly from borohydride solutions. Based on this, studies have been carried out using those elements. In 2000, Amendola [6] wrote a list of advantages of the $NaBH_4$ and throughout the years several researchers have written hundreds of articles, being the majority of them dedicated to the study of the catalysts reactivity [5], [10].

Recently, Demirci and Garin [11] and later Liu and Li [8] reviewed the most used catalysts. Besides that, it is worth to note some authors that studied the degradability and recyclability of the catalyst, as Kim *et al*. [12] that studied the degradation of filamentary Ni catalyst and reported a decrease hydrogen generation rate (*HGR*) after 200 cycles or Zhang *et al*. [13] that studied the durability of a supported catalyst using a fixed-bed reactor at various hydrogen demand conditions [1].

Also Peña-Alonso *et al*. [14] reported the study of *HGR* from stabilized $NaBH_4$ solutions with platinum and palladium and concluded that the catalyst is functional and has negligible degradation. Either Keçeli and Özkar [15] tested the durability of ruthenium (III) acetylonate as a catalyst [1].

Amendola *et al*. [16] studied a ruthenium based catalyst supported on ion exchange resin beads and achieved a high *HGR* with very small amounts of ruthenium. These results lead to the conclusion that is necessary to optimize the catalyst loading and support to be capable of generating large amounts of hydrogen. Regarding the catalyst of nickel and ruthenium, Pinto *et al*. [1] analysed this catalyst prior and, after 300 times of reutilisations to study its durability

and reutilisation capability, concluded that the *HGR* decreased proportionally to the number of times it was used , probably due to the segregation of ruthenium from the Ni-Ru alloy, which causes a decrease in the catalyst performance.

2.2 Hydrogen as an energy carrier

Hydrogen rarely exists in nature in its elemental state, so it cannot be considered as an energy source however, it has an energy density of 142 kJ g^{-1}, which is around three times higher than the energy density of petroleum (47 kJ g^{-1}), hence hydrogen can be considered as an energy carrier [17].

Although the molecule of hydrogen is the smallest in the world, this element is also the most abundant and it is colourless, odourless and tasteless. Table 2 presents some properties of hydrogen [18].

Table 2 - Properties of hydrogen. Adapted from [18].

Property	**Value**
Name / Symbol / Number	Hydrogen / H / 1
Category	Nonmetal
Atomic mass (u)	1.008
Electrons / Protons / Neutrons	1 / 1 / 0
Colour / Odour	Colourless / Odourless
Toxicity	None, simple asphyxiant
Phase	Gas
Density (g cm^{-3})	Gas: 8.99×10^{-5} / Liquid: 0.07
Ionization energy (eV)	13.5989
Liquid to gas expansion rate	1:848 (atmospheric conditions)
Melting point (ºC)	−259.14
Boiling point (ºC)	−252.87
Lower heat value (MJ kg^{-1})	118.8
Adiabatic flame temperature (ºC)	2107
Flammability range in the air (%)	4 - 75
Laminar flame velocity (**m s^{-1}**)	3.06
Flash point (ºC)	-253
Auto ignition temperature (ºC)	585
Research octane number	>130

Hydrogen can be generated from renewable or non-renewable sources, therefore it can have non-pollutants characteristics, as it can be clean and limitless since it comes from a renewable source, which makes the energy cycle sustainable and enrich the current green policies worldwide. However, the main resource for industrial mass scale hydrogen production is based on fossil fuels, since these fuels have a lower cost and are of easy usage in machine. Nowadays, the most economical method is steam-methane reforming and it represents the largest share in global hydrogen production [17], [18].

Despite this fact, a hypothetical idea of a hydrogen economy was developed, where fuels containing carbon would be replaced by hydrogen, to reduce air pollution and CO_2 growth in the atmosphere. To apply this concept means that the hydrogen would be used to store and transport energy from renewable sources over large distances [19], [20]. A good example of a country that has already started the transformation into a hydrogen economy is Iceland, that has abundant hydro and geothermal energies and plans to convert the country's fleet of cars, buses, etc. to hydrogen and thereafter use the hydrogen generate electricity and provide heat and power to its buildings [2], [21].

Since hydrogen is just an energy carrier, it is necessary to convert the hydrogen into energy, using either direct combustion in internal combustion engines or in proton exchange membrane fuel cells (PEMFC) [21]. The most promising application of hydrogen is the fuel cell, as it needs hydrogen as fuel to generate energy, and implies zero emissions at the local level. A fuel cell is a device that produces electricity from chemical energy and has the advantages of being more efficient than combustion engines, not having moving parts, with potential for highly reliable and long-lasting systems; and it is a silent device. Among the various types of fuel cells, PEMFC is the most suitable for transport utilizations as they operate at low temperatures and have a high power density [22], [23]. In Figure 1, a scheme of the application of fuel cells in the concept of hydrogen economy is shown.

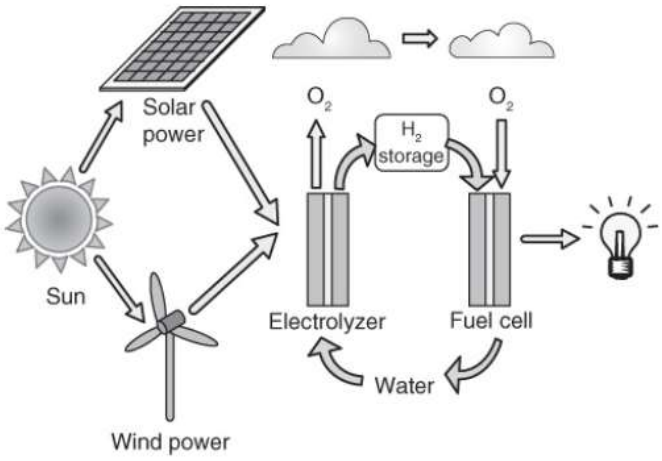

Figure 1 - Scheme of the application of fuel cells in the hydrogen economy [22].

One of the big issues of working with hydrogen is the storage conditions. Hydrogen can be stored by compression (gas or liquid): as a gas, it is stored in high-pressure tanks typically at 350-700 bar; while liquid, hydrogen requires cryogenic temperatures, since the boiling point of hydrogen is -252.87 ºC at atmospheric pressure [24]. As an example, if compressed cylinders at 200 bar are used it will be necessary a volume of 225 L to store 4 kg of gaseous hydrogen, which would require too much space to practical transport applications. In the case of storage at higher pressures, up to 450 bar, it is necessary a reinforcement in the cylinders, which increases the mass of the system to a point which hydrogen only occupies a small percentage of its total weight [17]. Figure 2 displays a scheme with the different methods of hydrogen storage.

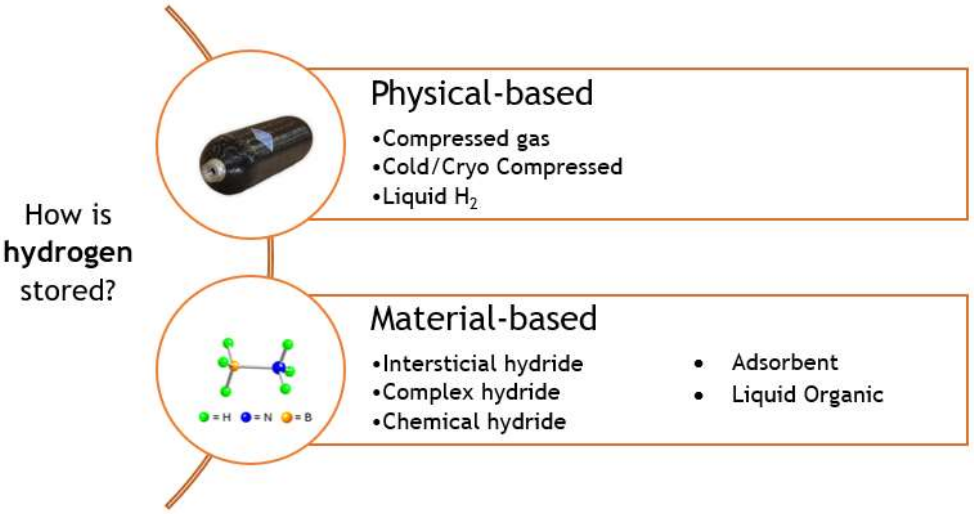

Figure 2 – Scheme of methods for hydrogen storage. Adapted from [24].

2.3 Chemical hydrides – the case of sodium borohydride

The most viable alternative to compressed or liquefied hydrogen is the storage of hydrogen in solids, since they demonstrate higher energy density than liquid hydrogen. Two examples are the metal hydrides, formed from alloys as $NaAlH_4$, or the chemical hydrides, as MgH_2 or NH_3BH_3 [25].

Sodium borohydride is contemplated as a possible compound to store hydrogen, due to its high gravimetric and volumetric hydrogen storage capacities [5]. Millennium Cell Inc. was a development stage company that developed hydrogen batteries for use in portable electronic devices for several markets, including the military. It was the first company to design a prototype of a hydrogen gas generator using aqueous sodium borohydride solution and ruthenium catalyst. Amendola *et al.* [6], [16] worked at Millennium Cell Inc. and published two papers about their prototype promising a safer and more controllable reaction with a possibility of adaptation to vehicular applications, where $NaBH_4$ could be carried on-board and stored in light-weight plastic tanks. Nevertheless they admitted that it would only be commercially successful if the cost of $NaBH_4$ decreased [26], [27].

However, in 2007, the U.S. DOE communicated that the hydrogen storage technology considered for the hydrolysis of $NaBH_4$ didn't reach the 2007 targets and recommended a no-go decision. Besides not having achieved the targets, the other reasons behind this decision were the high cost of net system due to the energy requirements, the high amount of energy needed and cost of recycling the sodium borate and its accumulation. Moreover, the overall efficiency of the regeneration process remains lower than the U.S. DOE goal of 60 % [28]. The DOE's targets for hydrogen storage systems, for portable equipment of medium power, between 2.5 and 150 W are shown in Table 3.

Table 3 – DOE's technical targets for medium power portable equipment using hydrogen as fuel [29].

Storage parameters	**Units**	**2015**		**2020**	
		Single-use	Rechargeable	Single-use	Rechargeable
Hydrogen Capacity	g_{H_2}	>1 - 50			
System gravimetric capacity	kWh kg^{-1} ($kg_{H_2} kg^{-1}_{system}$)	0.7 (0.02)	0.5 (0.015)	1.3 (0.04)	1.0 (0.03)
System volumetric capacity	kWh L^{-1} ($kg_{H_2} L^{-1}_{system}$)	1.0 (0.03)	0.7 (0.02)	1.7 (0.05)	1.3 (0.04)
System cost	\$ per Wh_{net} (\$ per $g_{H_2\ stored}$)	0.2 (6.7)	1.0 (33)	0.1 (3.3)	0.5 (17)

Furthermore, in Figure 3 it is possible to observe the ultimate targets of gravimetric and volumetric capacities imposed by DOE, which are 70 $g_{H_2} L^{-1}$ and 7.5 wt%, and it is also represented the current capacities for different types of hydrogen storage. Since the $NaBH_4$ is a chemical hydride, its capacities are still below the target. It is important to note that the *GHSC* is usually calculated only based on $NaBH_4$ and water, while it must be calculated based on the complete storage system, including all the equipment, as reactors or tanks [30].

Sodium borohydride reacts with water and forms hydrogen and sodium borate according to the reaction shown in equation 2.1, where *x* represents the excess hydration factor [31]. This reaction occurs even without catalyst if the pH of the solution is less than 9, therefore the

$NaBH_4$ solutions are typically maintained as alkaline solutions by adding NaOH, in order to increase the shelf life of $NaBH_4$ and to prevent the production upon standing of H_2 gas [6].

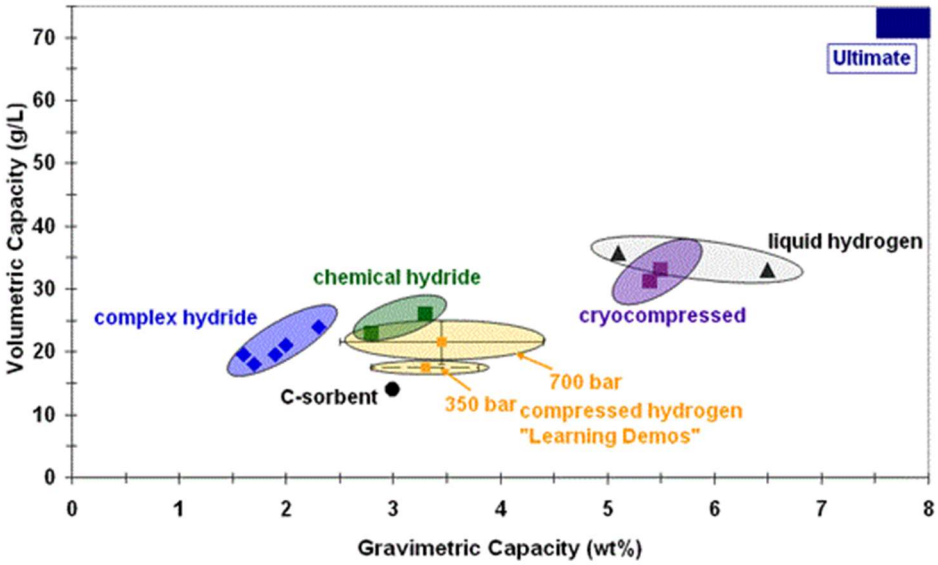

Figure 3 - Gravimetric and volumetric capacities for different types of hydrogen storage. Adapted from [32].

$$NaBH_4 + (2+x)\ H_2O \rightarrow NaBO_2 \cdot x\ H_2O + 4H_2 + \text{heat} \qquad (2.1)$$

The ideal hydrolysis is obtained for *x* equal to 0, where two moles of water react with one mole of $NaBH_4$ to produce four moles of hydrogen. However, it is necessary to have excess of water so the by-product exists with varying degrees of hydration, since its hydrated form is the stable one and also because at higher concentrations the precipitation of $NaBO_2$ could degrade the catalytic performances [5], [33].

In Figure 4 an evolution of *GHSC* of the fuel [$NaBH_4$ + (2+*x*) H_2O] with the excess of water is given and it shows that the *GHSC* increases with the reduction of *x*. Nevertheless, when *x* is higher, the *HGR* increases and that is why efforts to optimise the $H_2O/NaBH_4$ molar ratio have been made [5].

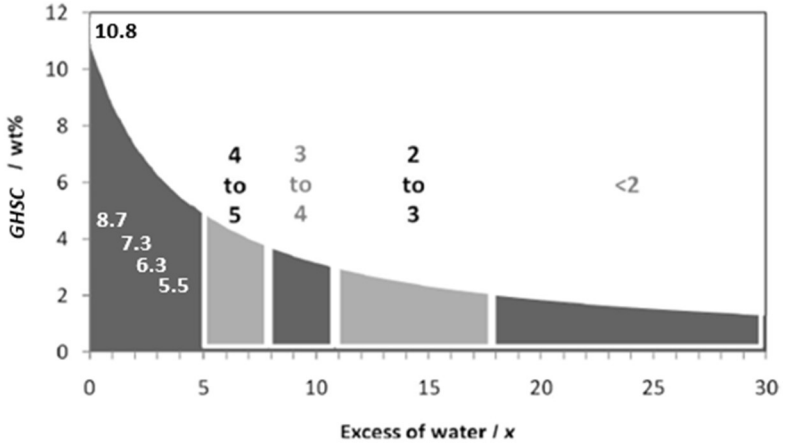

Figure 4 – Evolution of GHSC of the fuel [$NaBH_4$ + (2+x) H_2O] with the excess of water. Adapted from [5].

2.4 Catalysts for $NaBH_4$ hydrolysis

It is known that increasing the pH of the $NaBH_4$ solution over time inhibits the hydrolysis reaction, then, at room temperatures, only a small percentage of the theoretical amount of hydrogen is released by hydrolysis reaction of $NaBH_4$ and water. However, the generation of hydrogen can be enhanced by using catalysts [17], [34].

According to Demirci [10], between 2000 and 2013, 98 % of the articles dedicated to catalysis in the hydrolysis of sodium borohydride, were focused on heterogeneous catalysts and the remaining 2 % in homogeneous catalysts, on a list containing more than 300 catalysts. The most researched element is cobalt, due to its high catalytic activity and cheapness, in addition, ruthenium and nickel were also studied in detail.

The most common method to prepare a non-noble metal catalyst in powder form is by impregnation-chemical reduction, yet these powder catalysts have the disadvantages of being easy to aggregate and difficult to be recovered. On the other hand, ruthenium, platinum and other noble metals have shown an excellent catalytic activity to accelerate the *HGR*, although they have a high cost and are not easily available [35].

Another way of using a catalyst is in a supported form, which is suitable for practical applications, since it prevents the aggregation of catalyst particles into larger particles, when compared with the powdered catalysts and their salts, thus improving the catalytic activity and lifetime. The usual method used in its preparation is the surface impregnation followed by reduction treatment using either reducing solvents or hydrogen. This method is well established although the adhesion between the catalyst and the support continues to be studied, in order to improve its durability and strength [36].

A literature overview for noble transition metals catalysts is presented in Table 4, where is possible to observe that with the use of ruthenium-based catalyst highest values of *HGR* are reached. As shown in Table 4, the highest rates obtained were 96 800 $mL_{H_2} min^{-1} g_{Cat}^{-1}$ with the Ru(0) nanoclusters, reported by Özkar and Zahmakiran [37], followed by Ferreira *et al*. [31] that reported a *HGR* of 87 400 $mL_{H_2} min^{-1} g_{Cat}^{-1}$, using a Ni-Ru catalyst. Most of the results were obtained with atmospheric pressure.

Furthermore, the highest *HGR* achieved until now was reported by Zhuang *et al*. [38] which obtained 113 100 $mL_{H_2} min^{-1} g_{Cat}^{-1}$ in the production of 6.43 wt% H_2 by sodium borohydride hydrolysis at room temperature with a Co-Mo-B catalyst, a non-noble metal catalyst.

Table 4 - Literature overview ***for noble metal catalysts*** *for sodium borohydride catalysis, adapted from* [30], [39].

Catalyst	Form	Catalyst / Support (Amount /g, Loading/wt%)	Reuse	E_A (kJ mol^{-1})	*HGR* ($mL_{H_2} min^{-1} g_{Cat}^{-1}$)	$NaBH_4$ Concentration (wt%)	Temperature (ºC)	Year	Ref.
Ru	Supported on IRA 400 resin	0.25 g / 5.00 wt%	n/a	56.00	189	20.0	25	2000	[16]
Pt-$LiCoO_2$	Powder	0.26 g / 1.50 wt%	n/a	n/a	3 100	20.0	22	2002	[40]
Pt/C	Powder	0.10 g / 20.00 wt%	0	n/a	23 090	10.0	Not stated	2004	[41]
Ru(0) nanoclusters	Powder	n/a	0	28.51	96 800	0.8	25	2005	[37]
Pt/Ru-$LiCoO_2$	Catalyst dispersed on a nickel mesh	0.13 g / 10.00 wt%	n/a	n/a	2 400	5.0	25	2005	[42]
Pt/C	Powder	1.00 g / 13.10 wt%	n/a	n/a	23 000	10.0	25	2006	[43]
Ru(0) nanoclusters	Powder	n/a	n/a	41.00	4	0.6	25	2006	[44]
Pt/C	Powder	5.00 wt%	n/a	45.00	6 000	9.0	25	2007	[45]
Pt/Pd-CNT	Supported on CNT paper	4.70×10^{-3} g	20	19.00	126	0.1	29	2007	[14]
Pt/C	Powder	0.25 g / 2.00 wt%	n/a	n/a	170	5.0	30	2007	[46]
Ru/C	Powder	0.20 g / 3.00 wt%	0	83.50	770	1.0	25	2007	[47]
Rh/TiO_2	Supported on TiO_2	1.00 wt%	0	n/a	1 820	0.5	40	2007	[48]

$Ru_{60}Co_{20}Fe_{20}$	Supported on activated carbon fibers	2.50×10^{-3} g	n/a	44.01	5 030	10.0	25	2008	[49]
Ru	Powder	0.01 g	n/a	n/a	18 600	5.0	60	2008	[50]
Ru-Pt/TiO_2	Powder	1.00 wt%	n/a	n/a	150	2.0	20	2008	[11]
Pt/$LiCoO_2$	Catalyst bed	0.02 g / 1.00 wt%	n/a	70.40	3 000	10.0	25	2008	[51]
Ru/$LiCoO_2$	Catalyst bed	0.02 g / 1.00 wt%	n/a	68.50	2 700	10.0	25	2008	[51]
Ru	Supported on ion exchange resin beads	0.20 g / 1.00 wt%	0	49.72	132	5.0	25	2008	[52]
Ru	Supported on polymer beads	0.10 g	n/a	n/a	216	1.0	Not stated	2009	[53]
Ru(0) nanoclusters confined in zeolites	Powder	0.80 wt%	0	49.00	130	1.1	25	2009	[54]
Ru	Supported on graphite	0.30 g / 3.00 wt%	n/a	61.10	969	10.0	30	2010	[36]
Rh/TiO_2	Supported on TiO_2	6.00 wt%	n/a	n/a	210	15.0	23	2010	[55]
Ni-Ru	Powder	0.48 g / 1.42 wt%	150	n/a	24 200	10.0	25	2010	[4]
Ni-Ru	Powder	0.48 g / 1.42 wt%	266	n/a	33 000	30.0	25	2011	[1]
Ni-Ru	Powder	0.24 g / 1.42 wt%	320	n/a	87 400	45.2	25	2012	[31]

Ru composite	Supported on alumina	0.50 g	n/a	n/a	68	12.5	25	2012	[56]
Ru/C	Powder	0.10 g / 2.00 wt%	n/a	53.40	570	10.0	25	2012	[57]
Ru-RuO_2/C	Powder	0.01 g / 6.13 wt%	n/a	n/a	2 800	5.0	30	2013	[58]
Ru nanoparticles	Supported on $Ti_3C_2X_2$ [2]	6.99 wt%	0	22.10	59 040	1.0	25	2014	[59]
Ni-Ru	Powder	0.02 g	47	75.12	57 120	46.0	55	2014	[30]
Ni-Ru	Powder	0.48 g / 1.42 wt%	50	n/a	980	10.0	25	2016	[60]
Ru(0) Nanoparticles	Supported on xonotlite nanowire	1.37 wt%	n/a	75.00	1 110	0.4	25	2016	[61]

[2] X = OH or F

Currently, the development of noble metal catalysts is slower than a few years ago. However, in the non-noble metal catalysts research area, in 2017, Tang *et al.* [62] reported a *HGR* of 33.2 $mL_{H_2}min^{-1}$ using Co nanoparticles supported flexible foam Co-F and Wang *et al.* [63] described a $NaBH_4$ hydrolysis accelerated by zinc chloride without catalyst and they achieved a *HGR* of 1 933 mL_{H_2} g^{-1} in 120 min.

2.5 Different types of reactors

The most regular geometry in reactors is cylindrical, with conical or flat bottom, being that some studies were made to improve the shapes and geometries of the reactors, in order to increase the *HGR*. Ferreira *et al.* [4] reported a H_2 yield of 86 % and 98 % for conical bottom reactors with 369 cm^3 and 229 cm^3 of volume, respectively, while with a flat bottom reactor of 646 cm^3 it was obtained a H_2 yield of 78 %. Thus, the authors conclude that a conical bottom reactor increases both *HGR* and hydrogen yield, comparing with a flat bottom reactor.

Later, the same researchers [64] wrote about the accumulation of condensed water from its evaporation on the top of the reactor at the end of the experiments. This phenomenon can be one of the factors accountable for the non-complete reaction of hydrogen generation, since it reduces the quantity of water available in the reaction medium [30].

Therefore, it was optimized a geometry to an ovoid mini-reactor, using AISI 316L stainless steel, designed for portable applications, with an internal volume of 9 cm^3. With this reactor, Nunes *et al.* [60] reported a 90 % H_2 yield with 10 wt% of $NaBH_4$ solution and 7 wt% of NaOH. This optimized reactor, which will be used to carried out the experiments of this thesis, is represented in Figure 5. Besides the mini-reactor, it is also represented an input/output valve (V), a thermocouple (T), a pressure probe (P) and a data acquisition system.

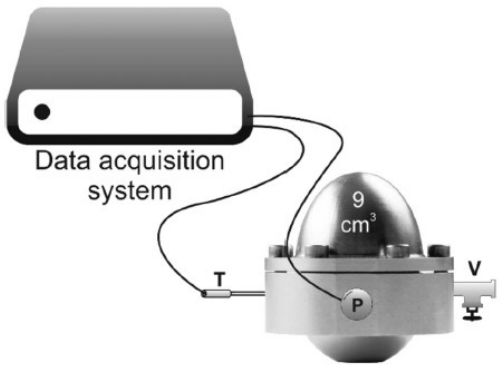

Figure 5 – Scheme of a typical experiment apparatus for hydrogen generation from $NaBH_4$ hydrolysis using the mini-reactor [60].

2.6 Proton Exchange Membrane Fuel Cells

As previously mentioned, a fuel cell is an electrochemical device in which the chemical energy is directly converted into electrical energy. It has two electrodes, anode and cathode, where electrochemical reactions occur, producing electrons at the anode which pass through an electric circuit to the cathode [65], [66]. This process is more efficient and quiet than the equivalent-power thermal generator and it can be used either for applications in buildings due to its compact design, such as small distributed power generator, or in portable applications, as laptops or mobile phones, since it has a longer operating and faster response time compared to batteries [67]. The characteristics of the main types of fuel cells are summarized in Table 5.

Table 5 – Summary of the different types of fuel cells [68].

Fuel Cell	Temperature (°C)	Efficiency (%)	Application	Advantages	Disadvantages
AFC	50-90	50-70	Space application	High efficiency	Intolerant to CO_2 in impure H_2 and air, corrosion and expensive
PAFC	175-220	40-45	Stand-alone and combined heat and power	Tolerant to impure H_2 commercial	Low power density, corrosion and sulphur poisoning
MCFC	600-650	50-60	Central, stand-alone and combined heat and power	High efficiency, near commercial	Electrolyte instability, corrosion and sulphur poisoning
SOFC	800-1000	50-60	Central, stand-alone and combined heat and power	High efficiency and direct fossil fuel	High temperature, thermal stress failure, coking and sulphur poisoning
PEMFC	60-100	40-50	Vehicle and portable	High power density, low temperature	Intolerant to CO_2 in impure H_2 and air and expensive.
DMFC	50-120	25-40	Vehicle and small portable	No reforming, high power density and low temperature	Low efficiency, methanol crossover and poisonous by-product

The beginning of fuel cells goes back to 1839 when Sir William Grove discovered that electricity could be generated by reversing water electrolysis. There are six main types of fuel cells with commercial importance and potential use in stationary and portable applications, which are

alkaline fuel cell (AFC), phosphoric acid fuel cell (PAFC), molten carbonate fuel cell (MCFC), solid oxide fuel cell (SOFC), proton exchange membrane fuel cell (PEMFC) and direct methanol fuel cell (DMFC) [30], [67].

Based on Table 5, it is possible to observe that PEMFC works at low temperatures, has a high-power density and a reasonable efficiency, which makes it the most promising fuel cell technology. The key factor of the fuel cell is the membrane electrode assembly (MEA) that is a thin layer placed in a sandwich structure of electrode-catalyst-membrane-catalyst-electrode [22], [30].

The PEMFC works with hydrogen and oxygen that are supplied to the anode and the cathode, respectively. A basic structure of a PEMFC is presented in Figure 6, where the operating principle is illustrated. At the anode hydrogen splits into electrons and protons. The splitted electrons provide the electrical output, while the protons flow through the electrolyte to the cathode to recombine with oxygen and produce water [22], [23], [30]. The electrochemical reactions occurring at the anode and the cathode are represented below:

Anode: $H_2 \rightarrow 2H^+ + 2e^-$ (2.2)

Cathode: $^1/_2\, O_2 + 2H^+ + 2e^- \rightarrow H_2O$ (2.3)

Overall reaction: $H_2 + {}^1/_2\, O_2 \rightarrow H_2O$ (2.4)

Usually, multiple cells of PEMFC are used stacked together to obtain a higher power system. This PEMFC stack has the cells attached in series to get a higher total voltage and in parallel to obtain a larger total current [67].

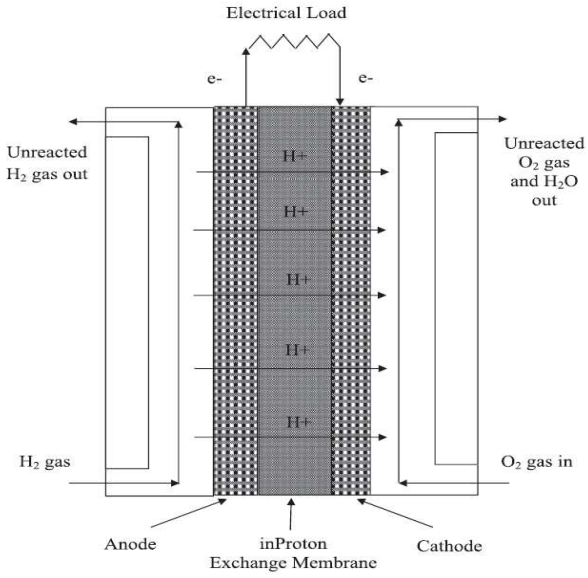

Figure 6 – Basic structure of a PEM fuel cell [67].

3. Materials and Methods

The materials used in the study of the effect of a Ni-Ru supported catalyst in the sodium borohydride hydrolysis are presented in this chapter, as well as the experimental setup and the procedure used.

3.1 Experimental setup

The experimental setup, represented in Figure 7, comprised the reactor which was connected to a data acquisition system. The data acquisition system was composed by two thermocouples (T_{in} and T_{out}), one pressure transducer (P) and the Labview software. The thermocouples, one installed inside the reactor and the other outside, were used to monitor the temperatures during the experiments. The internal thermocouple was used to observe the increase in temperature caused by the exothermic reaction, while the external thermocouple was to ensure the thermal isolation of the reactor, obtained by internal mirroring and geometry of the reactor. The pressure transducer, that worked inside the reactor, was calibrated from 0 to 40 bar and it measured the gas pressure inside the reactor until it reached a constant pressure plateau, which meant the end of the reaction. It is noteworthy that this measurement was fundamental to the quantification of *HGR* (Hydrogen Generation Rate) and the hydrogen yield, since both parameters are related to the pressure inside the reactor. Finally, all of the data acquired were recorded using the Labview software.

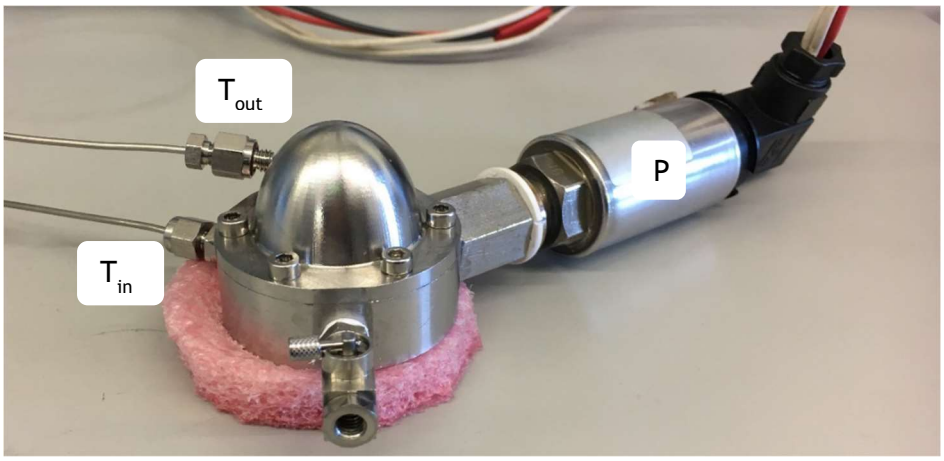

Figure 7 - Image of the mini egg-shaped reactor, used in the experiments.

3.1.1 Reactor

All the tests, with the exception of the first experiment to activate the catalyst, were carried out in the mini egg-shaped reactor, mentioned in Chapter 2. This reactor has an internal volume of 9 cm^3 and due to its size, it is suitable for portable applications, and its effectiveness was already proved by Nunes *et al.* [60].

3.1.2 Reactants

The anhydrous sodium borohydride used to perform the experiments was provided by Panreac (123314.1608), with 96 % of purity, and it was kept in the desiccator until use.

To carry out the alkali hydrolysis studies, the sodium borohydride solution was stabilized through the addition of small quantities of sodium hydroxide pellets, with 98 % of purity and supplied by EKA (No.: 1310.73.2).

3.1.3 Catalysts

The experiments were performed using the following catalysts: a powder unsupported Ni-Ru based catalyst and three Ru catalysts supported on a Ni foam with the Ru amounts of 2.04 mg, 0.95 mg and 0.44 mg. All catalysts were synthetized by *Laboratório Nacional de Energia e Geologia* (LNEG) in October 2017.

Ferreira *et al.* [4] described the preparation of a similar Ni-Ru based catalyst, unsupported, in a fine powder form. Briefly, it was prepared from an impregnation of a mixture of nickel and ruthenium salts (Riedel-de Haën) in deionised water, by chemical reaction with 10 wt% borohydride stabilized solution (Rohm and Haas), as the reducing environment. After that, the catalyst was appropriately decanted, washed, filtered, dried and heat-treated at 110 ºC.

Furthermore, the supported catalyst of Ru and Ni was prepared through electroplating, using a 5 M alkaline solution of KOH, with 2 mg mL^{-1} of $RuCl_3$ with 48 % of Ru, at room temperature, and a system of two electrodes, where the cathode was the working foam and the anode was a Ni foam. The electroplating was made with a potential of 5.4 V at a variable time, depending on the amount of catalyst planned to electroplate. Then, the foams were washed with distilled water and heat-treated at 100 ºC.

The support used was a nickel foam. These foams were washed in ethanol, in hydrochloric acid (with 10 wt%) and distilled water and, finally, dried at 100 ºC.

At the end of each experiment the catalyst was recovered for reutilization.

3.2 Catalyst characterization

The catalysts used in the experiments were analysed in CEMUP (*Centro de Materiais da Universidade do Porto*) through scanning electron microscopy (SEM) coupled with Energy Dispersive X-Ray Spectroscopy (EDX), using the equipment JEOL JSM 6301F/ Oxford INCA Energy 350 / Gatan Alto 2500 to obtain surface morphological images and the analysis of the components. Also, an X-Ray Diffraction (XRD) analysis was performed at LCA (*Laboratório Central de Análises*) of the University of Aveiro, using the diffractometer Philips X'Pert MPD using a Cu – K alpha wavelength of 1.5405980 Å and 1.5444260 Å.

3.2.1 Scanning Electron Microscopy Analysis

The SEM allows the observation and characterization of heterogeneous materials (that can be organic or inorganic) on a nanometre to micrometre scale, using a microscope that operates with a focused beam of high-energy to generate a variety of signals at the surface of solid specimens [69]. This type of analysis is the second type more employed (the first one is X-Ray Diffraction - XRD) in research articles to analyse the catalysts used in sodium borohydride hydrolysis [10].

As shown in Figure 8, the electrons used to form the SEM image can be secondary (SE) or backscattered (BSE). The backscattered electrons are primary electrons that have been scattered by sample atoms and the intensity of this backscattering is proportional to the mean atomic number of the atoms. The images produced by these electrons provide information on variations in sample composition, while the secondary electrons are used to compose the classic topographic images. Normally, the SEM is applied to generate high-resolution images of object shapes and to show spatial variations in chemical compositions [70], [71].

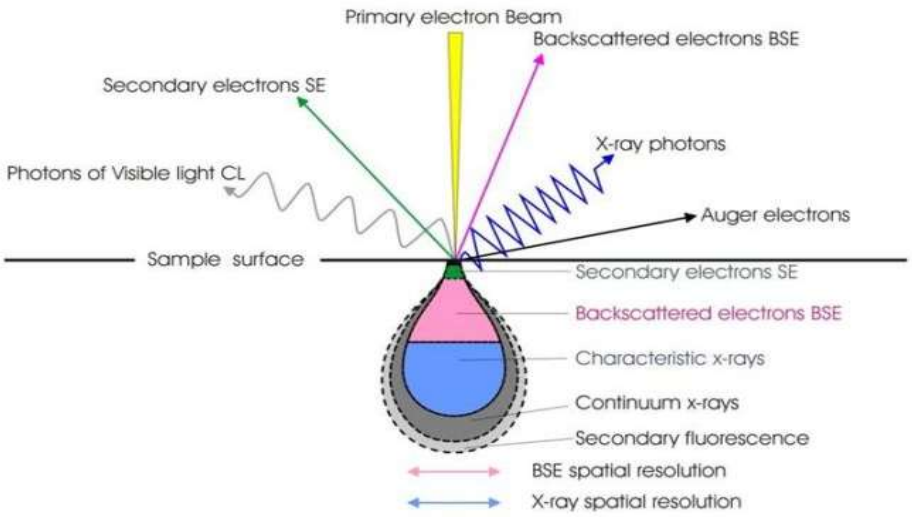

Figure 8 - Scheme of electrons scattering in a sample's surface [70].

In addition, Figure 9 shows the compounds of a scanning electron microscope presenting the electro gun that produces the steady stream of electrons necessary for the operation of SEM and the lenses that are used to produce a clear and detailed image. The condenser lenses control the spot size in the sample by converging the cone of the electron beam to a spot below, while the objective lens focuses the beam on a position. The SEM analysis is performed with vacuum, since without it the electron beam would be susceptible to a constant interference from air particles [72], [73].

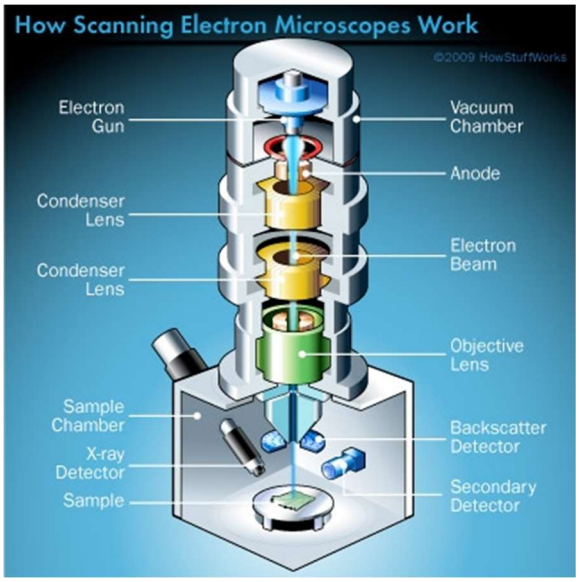

Figure 9 – Scheme of the components of a scanning electron microscope [72].

3.2.2 X-Ray Diffraction Analysis

The XRD analysis is the most described in research articles to analyse the catalysts used in sodium borohydride hydrolysis and it consists in a fast-analytical technique used for characterization of a crystalline material (mineral, inorganic, etc). This analysis allows the identification of distinct phases in the material, the determination of unit cells dimension, the measurement of sample purity, the sizes of grains and its micro-deformations and it can also be used to analyse more specifically some structures or determine measurements [10], [74].

The X-rays are generated by a cathode ray tube, filtered to produce monochromatic radiation and it is concentrated and directed to the sample, scattering on the atoms, as it is visible in Figure 10. However, the interactions between the X-rays and matter are different, so the X-rays can be scattered through an elastic or inelastic process by electrons. Additionally the geometrical constrains in the crystal structure will cause different directions and intensities in the diffraction of the beam [74], [75].

The principle of this technique is that the sample and the detector are rotated, and the intensity of the reflected X-rays is recorded. Once the geometry of the incident X-rays satisfies the Bragg equation, it occurs a constructive interference that leads to a peak in intensity. The detector records, processes and converts the X-ray signal to a count rate, that is outputted to a device [74].

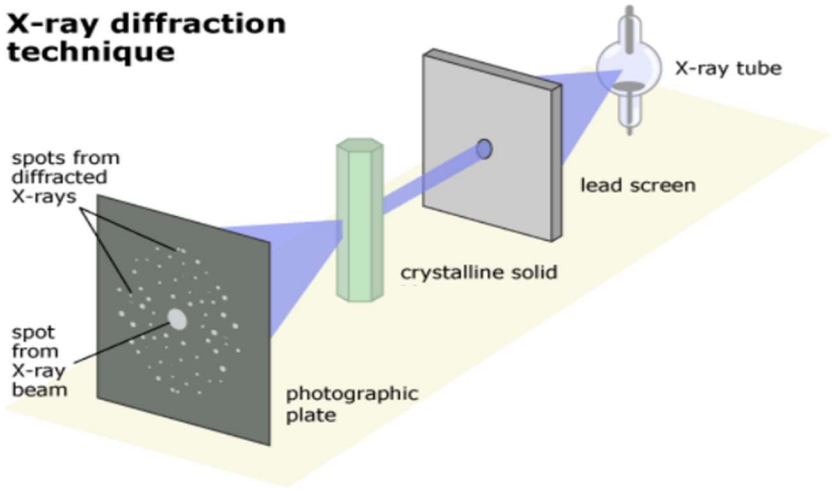

Figure 10 – Scheme of X-ray diffraction technique [76].

3.3 Experimental Procedure

This work was aimed to study the performance of a supported and unsupported catalysts. Firstly, it was necessary to perform a first experiment to activate the catalyst, since it was new.

Then, experiments were performed with the purpose of studying the parameter's influence in the hydrogen generation rate according to the catalyst used. The studied parameters were the hydration factor, temperature, catalyst/$NaBH_4$ mass ratio and the $NaBH_4$ amount. For the different parameters, four different types of catalysts, presented in Table 6, were studied in order to compare the results between each other and with the literature.

Table 6 – Types of catalysts used in this work.

Catalyst	Support	Amount of catalyst (mg)	Volume (cm^3)
Ni-Ru	Unsupported powder	-	-
ESPRU 1	Nickel foam	2.04	0.21
ESPRU 2	Nickel foam	0.95	0.22
ESPRU 3	Nickel foam	0.44	0.22

The procedure of all the experiments using a $NaBH_4$ stabilized solution (for a hydration factor of 16 or 11) was similar, starting with a preparation of the solution with 7 wt% of NaOH. To prepare these solutions, a specific amount of $NaBH_4$ was added to a certain volume of aqueous solution of NaOH and it was determined the density of each solution, using a pycnometer of 10 mL. As the solution is prepared, the catalyst was placed on the bottom of the reactor, which

was properly sealed, and the $NaBH_4$ stabilized solution was injected into the reactor, using a micro-syringe.

The procedure for the alkali-free experiments, using solid $NaBH_4$, consisted in the addition of $NaBH_4$ and the catalyst in the bottom of the reactor and, after sealing the reactor, the required amount of water was injected by a micro-syringe. These experiments were performed with a hydration factor of 0 and 2 and catalyst/$NaBH_4$ mass ratios range from 0.01 to 0.4 g/g.

The studies were performed at uncontrolled room temperature, excepting the study of the temperature influence. The powder catalyst was separated from the by-product of the reaction, washed with distilled water and decanted a few times to dissolve any remain of $NaBO_2$ and it was dried at 80 ºC for 1 hour, to enable its reutilization. While the supported catalyst foams were washed with distilled water and dried at 100ºC for 1 hour, thus they can be reused.

The experiments were carried out twice to almost all the studied conditions, in order to validate the results.

4. Results and discussion

This chapter is focused on presenting the analysis performed to the catalysts and the results obtained in several $NaBH_4$ hydrolysis experiments. The results are discussed and the influence of the parameters - hydration factor, temperature, catalyst/$NaBH_4$ mass ratio and the $NaBH_4$ amount - are studied. The performance of the several catalysts used was analyzed, as well as the hydrogen generation rates and yields. Finally, there is a comparison between the unsupported and supported catalysts and with the catalysts described in the literature.

It is noteworthy that the parameters referred in this chapter were calculated by the equations descripted in Appendix A.

4.1 Scanning Electron Microscopy images

The different catalysts were analyzed through SEM and the images obtained from the analysis are presented in Figure 11 and 12.

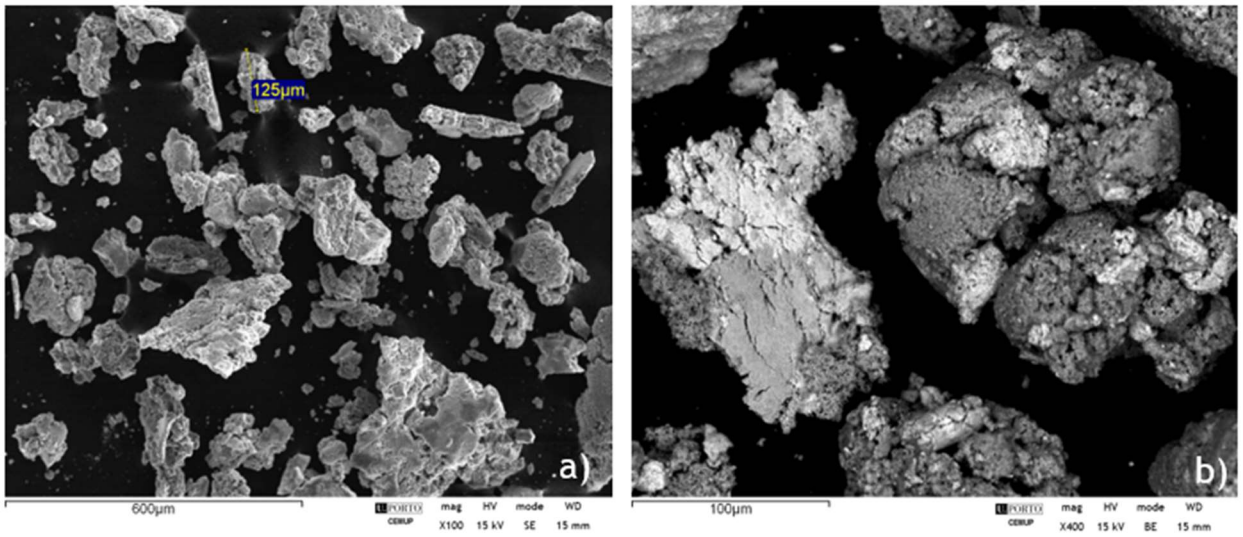

Figure 11 - SEM analysis of the unsupported catalyst in a powder form. a) Non-used catalyst, b) Catalyst reused once.

Figure 11 shows the SEM micrograph of the unsupported catalyst and it is evident that the catalyst is heterogeneous, with particles of different sizes and shapes. Moreover, the EDX spectra indicated the presence of the following elements: oxygen, nickel, ruthenium and carbon, as it is observable in Figure B.1 of the Appendix B. However, there were areas were the amount of ruthenium was residual, which leads to conclude that its distribution is not homogeneous. Between the non-used catalyst and the reused once, there were not significant differences in the morphology, as expected, which means that the experimental procedure was adequate.

The SEM analysis of the three supported catalysts are displayed in Figure 12. Since the support is the same, the images are similar, with the coating being the major differences. Thus, Figure

12 presents three images corresponding to the different catalysts, with different magnifications, showing that the support morphology is similar to a knit, where the ruthenium was deposited. In the images, it is perceptible that the zone around the pore is more damaged, showing flaws in the coating. Through the EDX spectrum, presented in Figure B.2, Appendix B, the elements found were oxygen, nickel (which was in the form of oxide and metal) and ruthenium.

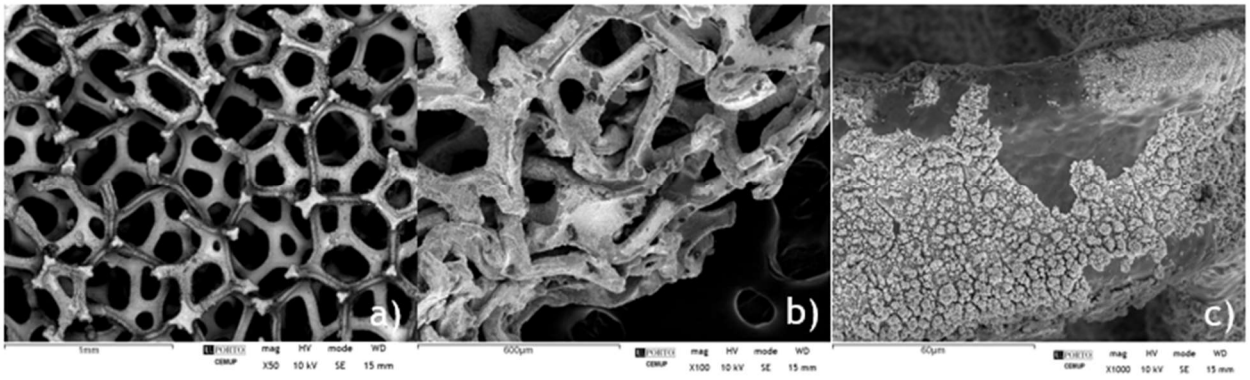

Figure 12 – SEM analysis of the supported catalysts. a) ESPRU 1 (foam with a catalyst amount of 2.04 mg), b) ESPRU 2 (with 0.95 mg of catalyst), c) ESPRU 3 (with 0.44 mg of catalyst).

4.2 X-Ray Diffraction Analysis results

The results obtained from the XRD analysis of the catalysts are exhibited in the Figures 13 and 14.

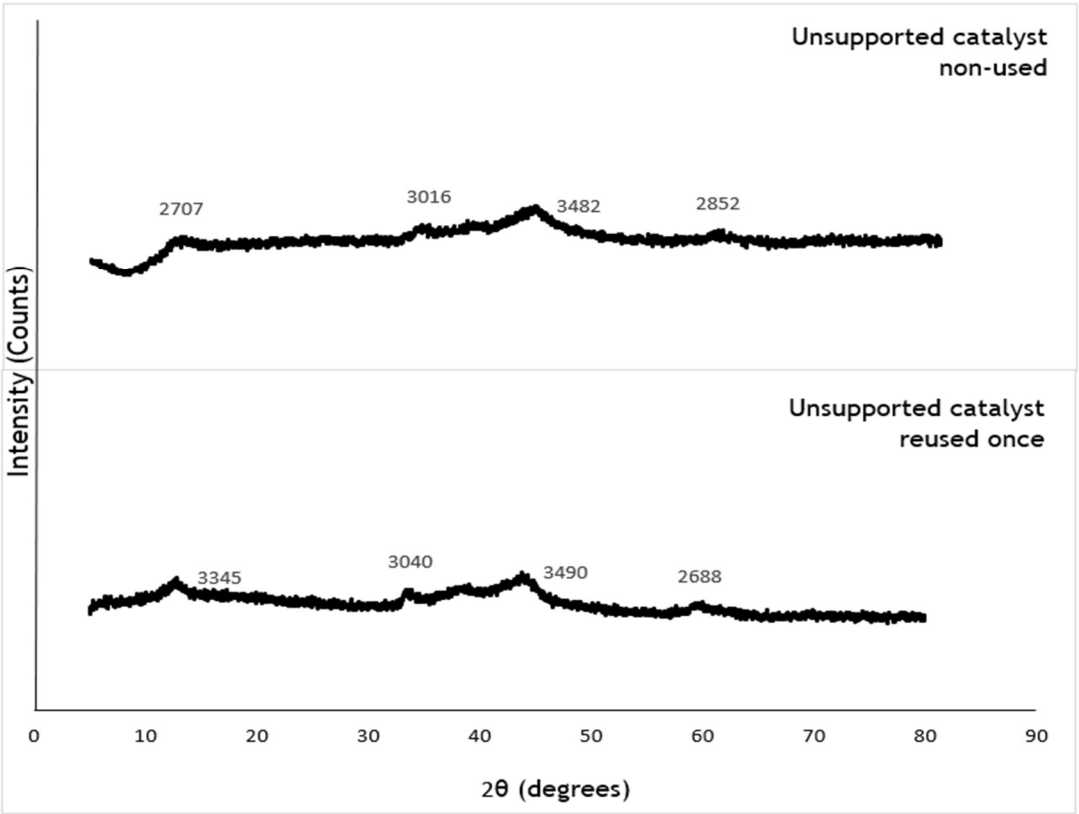

Figure 13 – XRD patterns of the unsupported catalysts, non-used and reused once.

Through Figure 13 it is perceptible that the patterns obtained for the unsupported catalyst non-used and reused once are very similar, with small peaks around 13, 34, 44 and 60 degrees. These patterns were analysed through Match! Software and the peaks were identified as belonging to nickel, ruthenium, carbon and oxygen. These results are in agreement with the elements found through EDX analysis and present in the spectra of Figure B.1, Appendix B.

Figure 14 shows the results of the XRD analysis for the three supported catalysts. As previously reported, the support of the catalyst is the same and, since the XRD analysis is qualitative, i.e. the amount of catalyst in the support did not influence the results, the patterns obtained for each supported catalyst were identical. Once again, the patterns were analysed through Match! Software.

Furthermore, Figure 15 demonstrates the pattern obtained by Huang *et al.* [77] for NiO nanosheet arrays on a Ni foam and, as can be observed, the strong peaks originating from that type of foam match with the peaks obtained in the patterns of the three supported catalysts at 44.5, 51.9 and 76.4 degrees - typical values of the nickel foam. Moreover, the peaks at 44.7, 52.1 and 76.5 degrees were reported by Huang *et al.* [78] in a study of a supercapacitor on Ni foam. Therefore, these peaks are respectively identified as (111), (200) and (220) planes of the Ni foam.

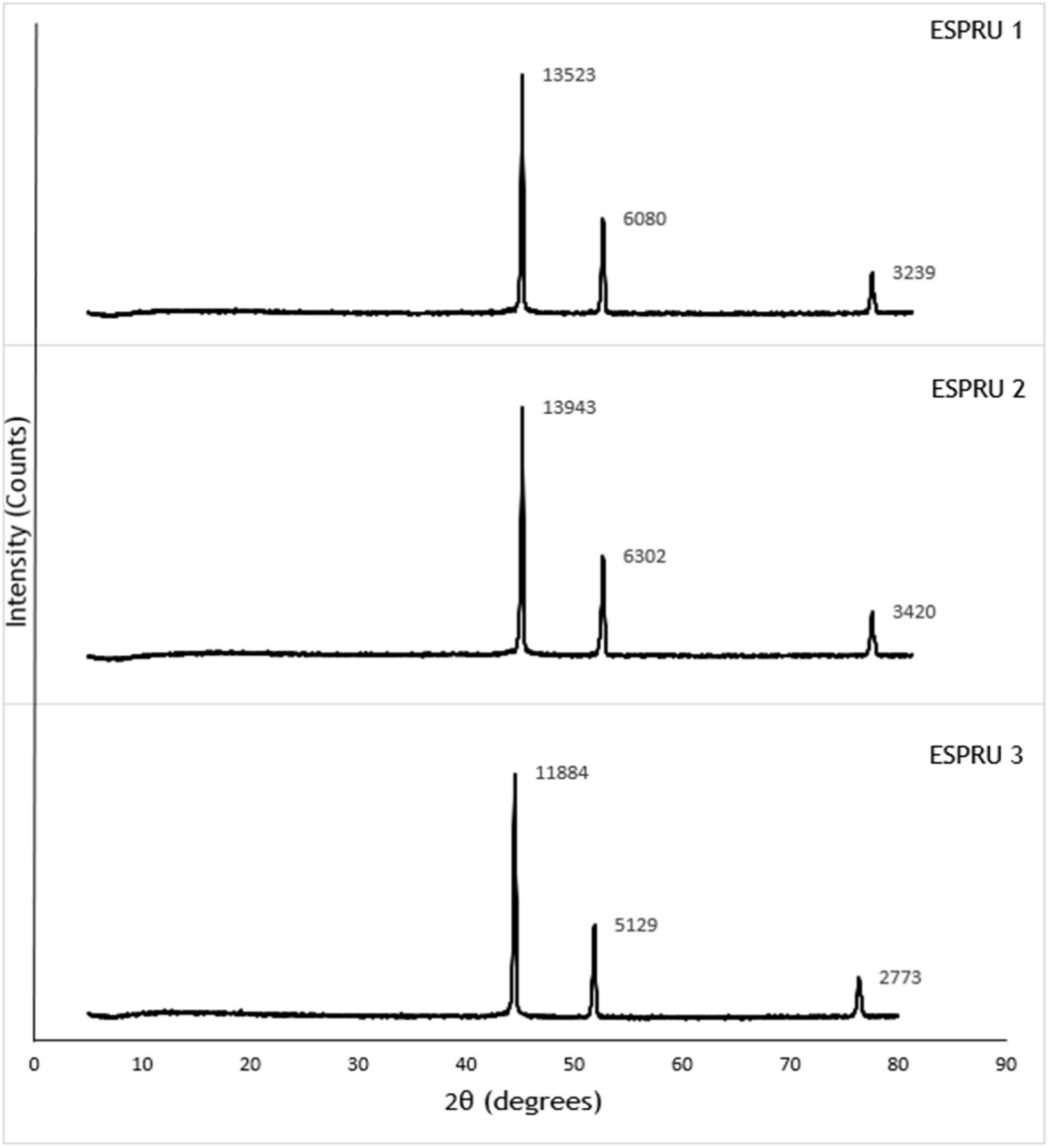

Figure 14 – XRD patterns of the three supported catalysts.

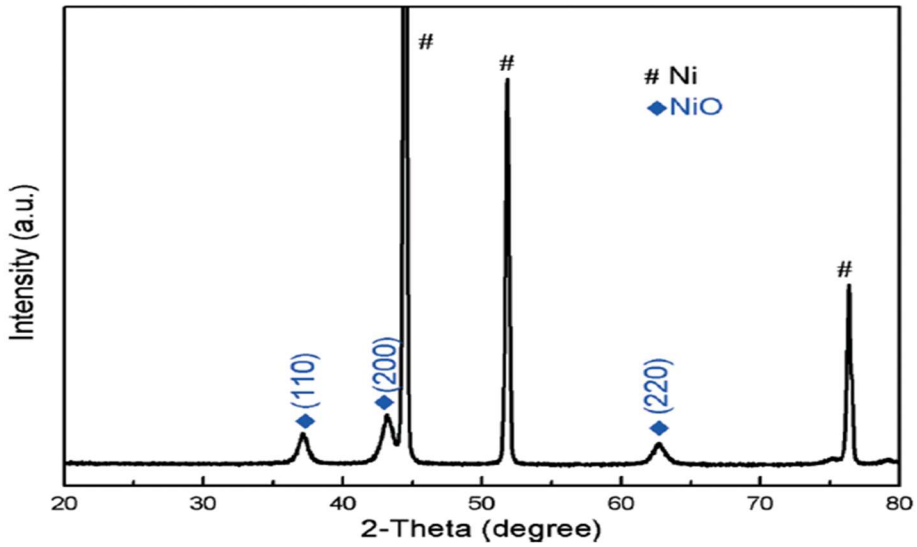

Figure 15 – XRD pattern of nanosheet arrays of nickel oxide on Ni foam [77].

4.3 Study of the unsupported catalyst

4.3.1 Activation of the catalyst

Most of the studies using a unsupported catalyst of Ni-Ru, to generate hydrogen by hydrolysis of sodium borohydride, were performed with a catalyst/$NaBH_4$ mass ratio of 0.4 g/g [1], [4], [60]. Therefore, the experiments were carried out with the same ratio, allowing a better comparison between the results.

Since the unsupported Ni-Ru catalyst used in this work was new, it was necessary to activate it first by performing a classic sodium borohydride hydrolysis reaction, at uncontrolled room temperature. In order to activate a higher amount of catalyst, this experiment was performed in a cylindrical reactor, with a flat bottom and a volume of 369 cm^3. Figure 16 plots the results of this experiment.

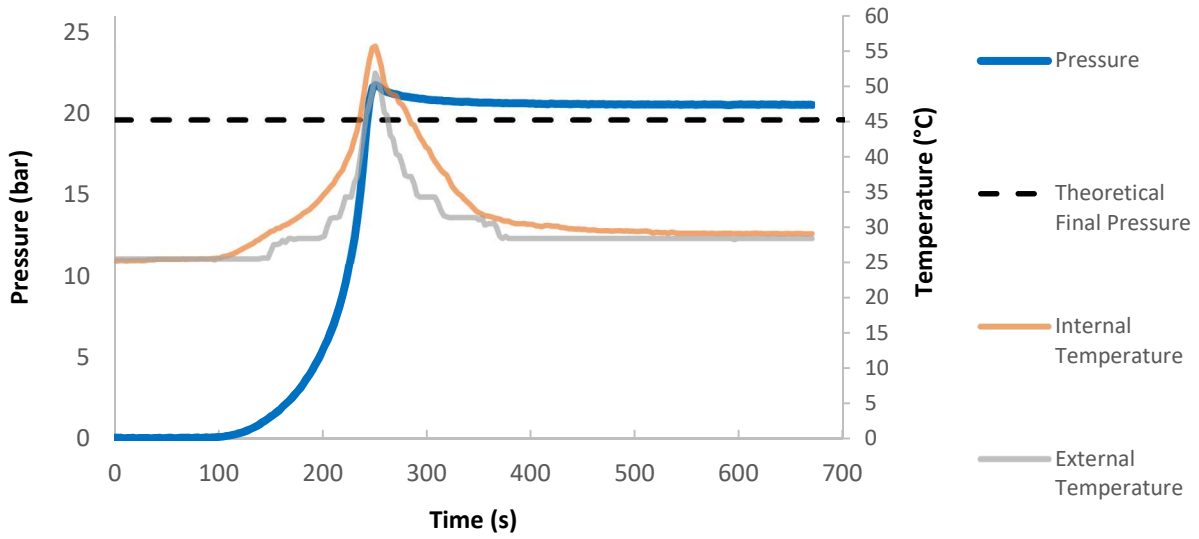

Figure 16 – Chart of hydrogen generation for a classic hydrolysis of sodium borohydride, at uncontrolled room temperature, with the purpose of activating the catalyst with the following conditions: m_{NaBH_4} *= 2.47 g,* m_{Cat}/m_{NaBH_4} *= 0.4 g/g and x = 16.*

Although the graphic shows an induction time higher than the usual, this fact can be easily explained since it was the first utilisation of the catalyst. In addition, the pressure increased during the time of experiment as it was expected, result of the hydrogen released. The results of this preliminary study, such as the yield, the *HGR* (calculated in STP conditions), the *GHSC* and the *VHSC* are presented in Table 7. The yield achieved was 100%, this value can be explained due to the fact that all the hydrogen produced was in the gas phase, which was detected by the pressure transducer.

Since this preliminary study was performed to activate the catalyst, it was not needed to replicate the experiment, as it is expected a performance similar to the descripted in the literature by Ferreira *et al.* [4], [31], [33], [64], Pinto *et al.* [1] and Nunes *et al.* [60].

Table 7 - Activation of the catalyst results.

m_{NaBH_4} (g)	η (%)	Induction time (s)	*dP/dt* (bar s^{-1})	*HGR* ($mL_{H_2} min^{-1} g_{Cat}^{-1}$)	*GHSC* (wt%)	VHSC (kg m^{-3})
2.47	100.00	127.00	0.63	13 125	2.29	25.20

4.3.2 Influence of the hydration factor

Nunes [30] studied the influence of the available quantity of $NaBH_4$ for the egg-shaped mini reactor with a catalyst/$NaBH_4$ mass ratio of 0.2 g/g and concluded that the value of 0.1 g of this reactant was more suitable for the experiments, since a higher yield, reaction rates and storage capacities were achieved. However, since the catalyst/$NaBH_4$ mass ratio for these experiments was stablished as 0.4 g/g, it was required to reduce the amount of $NaBH_4$ to 0.05 g.

The graphics for the several experiments carried out to study the influence of the hydration factor in the unsupported catalyst are shown in Figures 17 to 20, where *x* varied from 16 to 0. In the plots, the pressure and the reactor internal temperature versus time can be seen for the two experiments carried out with similar conditions, duly identified in the legends. It is also presented the theoretical final pressure however, since the two experiments had the same conditions, the theoretical final pressures were indistinguishable in the plots, hence it was only represented an average of both pressures. It is noteworthy that the reaction rates obtained in these experiments are reported in Table 8, presented in the next subchapter.

Furthermore, Nunes [30] verified that the inside and outside temperatures were practically constants through the reactions, validating the isolation of the reactor. Consequently, it was not necessary to represent the outside temperature in the plots.

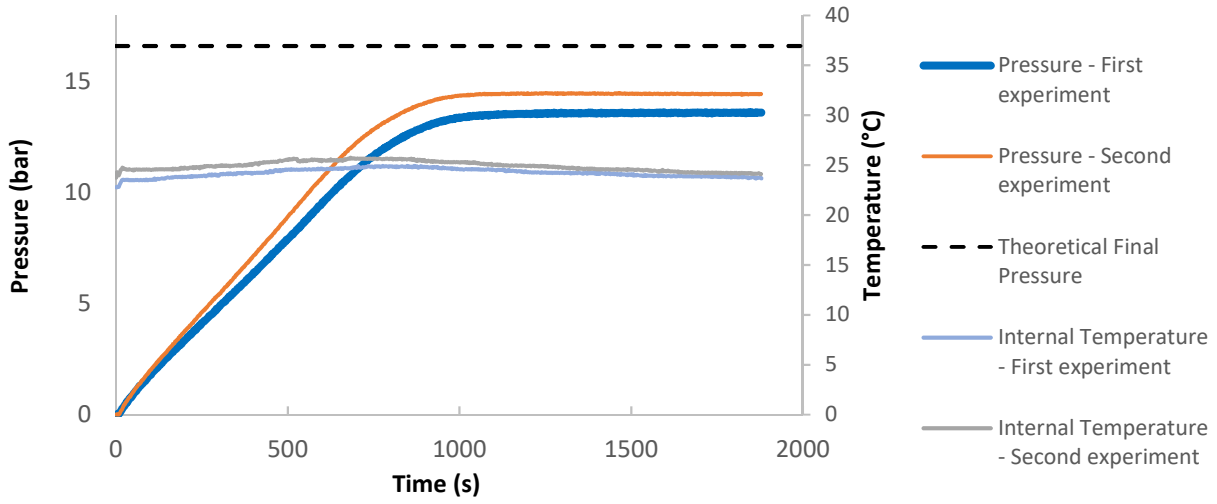

Figure 17 - Chart of hydrogen generation for a classic hydrolysis of sodium borohydride, at uncontrolled room temperature, to study the influence of the hydration factor with the following conditions: m_{NaBH_4} *= 0.052 g,* m_{Cat}/m_{NaBH_4} *= 0.4 g/g and* ***x = 16****.*

Through Figure 17 it is possible to observe that the pressure was higher in the second experiment and, as a result, the reaction yield was higher comparing with to the first experiment, 87.98 and 93.06 %, respectively. It is also perceptible that the internal temperature did not increase much with the beginning of hydrogen production. Although the results obtained in the second experiment were slightly higher (the temperature was 1 ºC higher), the experiments were consistent.

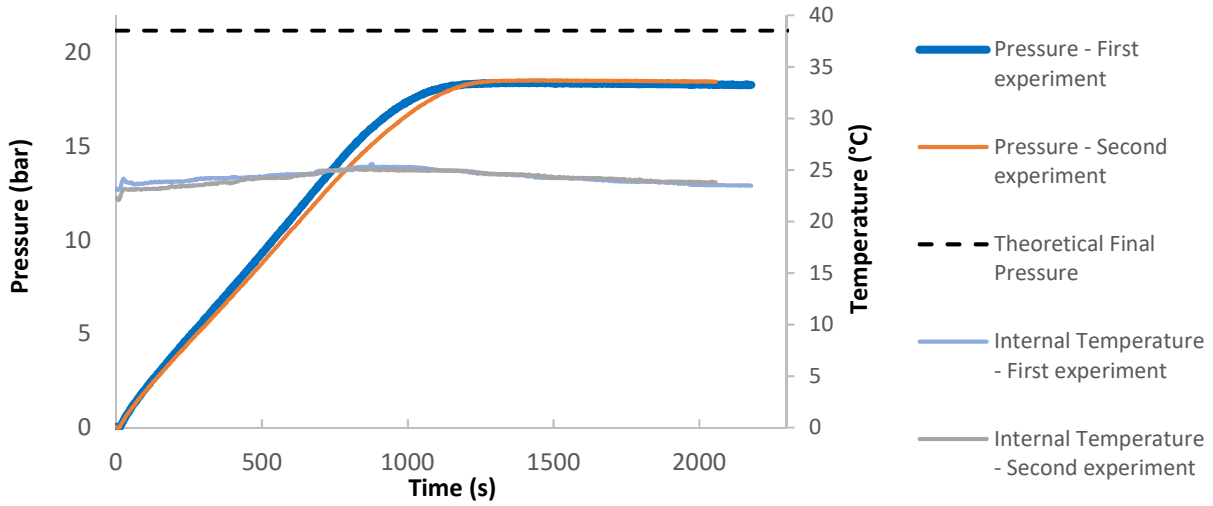

Figure 18 - Chart of hydrogen generation for a classic hydrolysis of sodium borohydride, at uncontrolled room temperature, to study the influence of the hydration factor with the following conditions: m_{NaBH_4} *= 0.067 g,* m_{Cat}/m_{NaBH_4} *= 0.4 g/g and* ***x = 11****.*

According to Figure 18, the experiments were concordant, and the results were similar. A yield of approximately 91.70 % in both experiments was reached together with a *GHSC* and a *VHSC* higher than the experiments with *x* equal to 16 as it was expected, since the amount of water in the solution was smaller. Once again, no significant change in the internal temperature was observed.

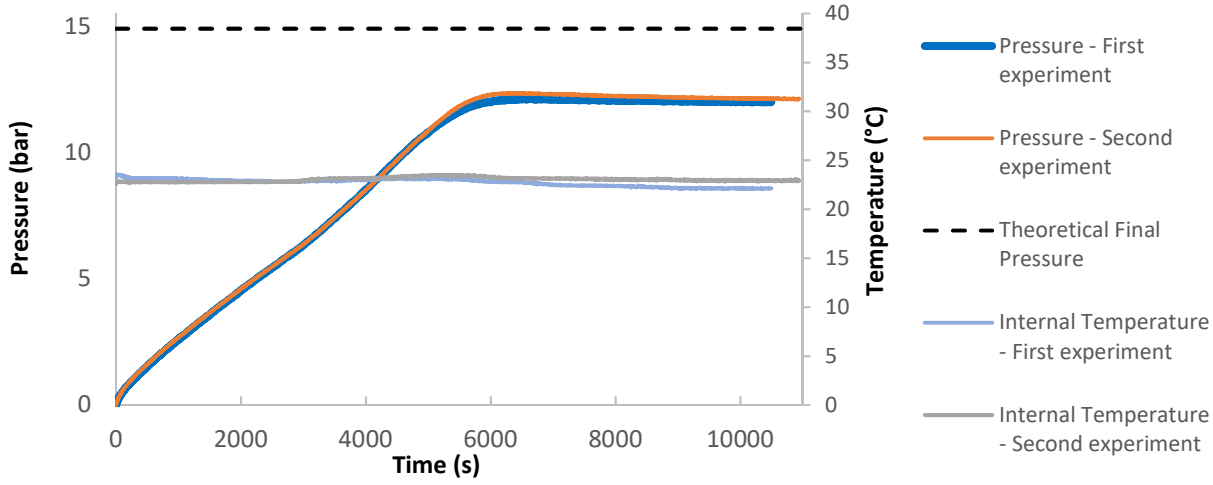

Figure 19 - Chart of hydrogen generation for an alkali free hydrolysis of sodium borohydride, at uncontrolled room temperature, to study the influence of the hydration factor with the following conditions: m_{NaBH_4} *= 0.048 g,* m_{Cat}/m_{NaBH_4} *= 0.4 g/g and* ***x = 2****.*

Figure 19 presents the plots of the experiments with a hydration factor of 2 and it is perceptible that the theoretical final pressure is lower than in the other experiments. Nevertheless, the reaction yields achieved were also lower, with values of 87.43 and 88.36 %, respectively. The induction time was lower, as it was expected, since the amount of water available in the reactor was lower. Moreover, the experiments were coherent, and the internal temperature did not have a significant variation.

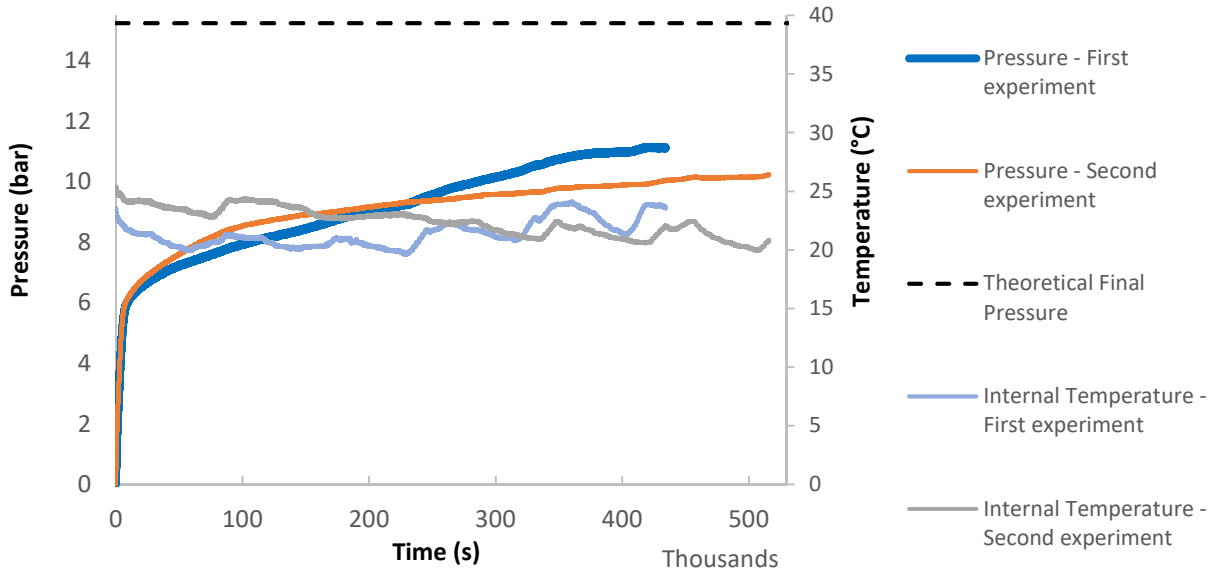

*Figure 20 - Chart of hydrogen generation for an alkali free hydrolysis of sodium borohydride, at uncontrolled room temperature, to study the influence of the hydration factor with the following conditions: m_{NaBH_4} = 0.048 g and 0.050 g, respectively, m_{Cat}/m_{NaBH_4}= 0.4 g/g and **x = 0**.*

In the plot represented in Figure 20 the X-axis stands-out due to its representation in thousands, meaning that the studies with a hydration factor of 0 were performed during approximately five days. Moreover, a high temperature variation over time can be noticed. This phenomenon is not surprising since the experiments were performed at uncontrolled room temperature, which was changeable during the days in operation and between the different times of day. In this experiment, for the hydrogen generation rates calculations, two distinct linear regions were considered (one with a higher slope value than the other).

Furthermore, since the experiments with *x* equal to 0 were performed with the minimum amount of water required, the *GHSC* and the *VHSC* were higher, nevertheless the generation of hydrogen was slower, not being feasible for a real application.

4.3.3 Influence of the temperature

The results of the hydrogen generation rate at uncontrolled room temperature were lower than the expected, which lead to the study of the $NaBH_4$ hydrolysis reaction at a higher temperature. Therefore, Figures 21 to 23 plots the pressure and internal temperature versus time for these

experiments, at a controlled temperature of 50 ± 5 ºC. It is noteworthy that despite the efforts to keep the temperature constant, this was not always possible with the equipment available.

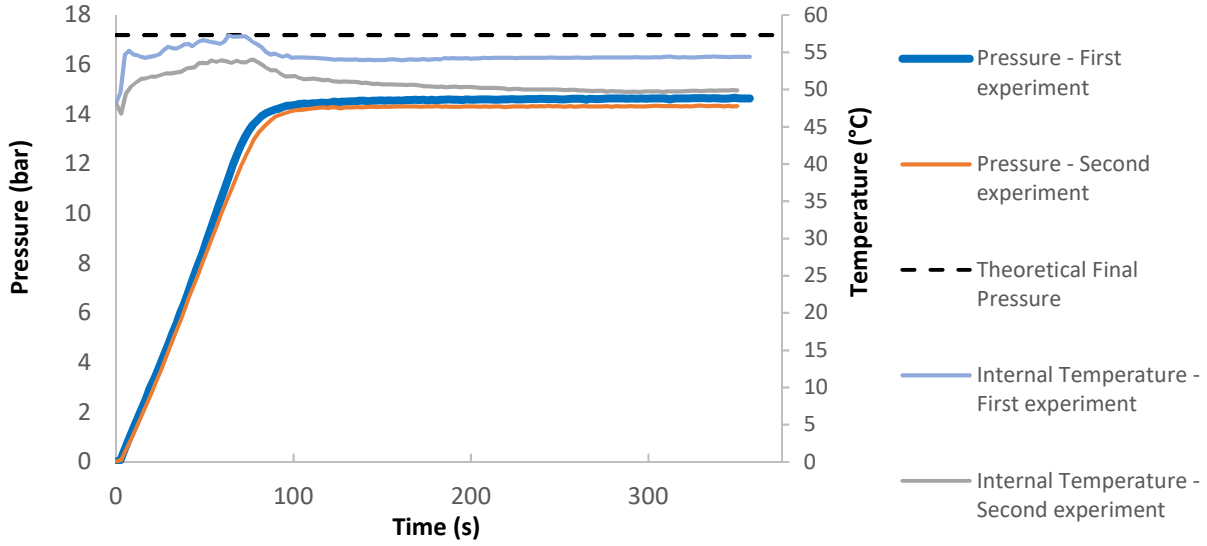

*Figure 21 - Chart of hydrogen generation for a classic hydrolysis of sodium borohydride, at 50 ± 5 ºC, to study the influence of the temperature with the following conditions: m_{NaBH_4} = 0.052 g, m_{Cat}/m_{NaBH_4}= 0.4 g/g and **x = 16**.*

In Figure 21 it is noticeable that the internal temperature increased more significantly during the hydrogen production than at room temperature studies. Comparing to the experiments at same conditions and uncontrolled room temperature, the results at 50 ºC present lower induction time and higher hydrogen generation rate.

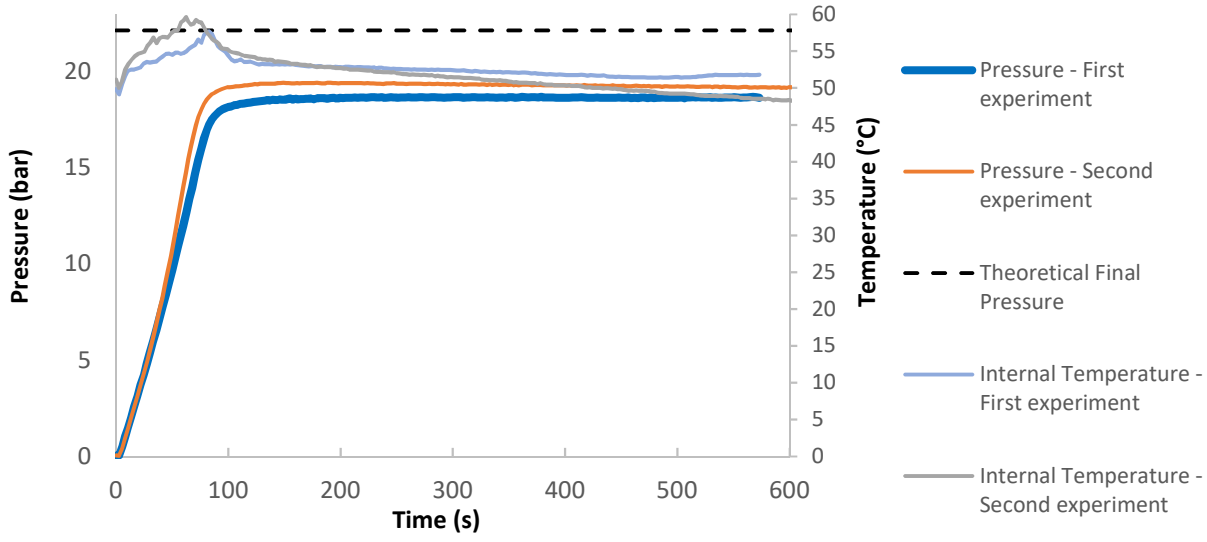

*Figure 22 - Chart of hydrogen generation for a classic hydrolysis of sodium borohydride, at 50 ± 5 ºC, to study the influence of the temperature with the following conditions: m_{NaBH_4} = 0.067 g, m_{Cat}/m_{NaBH_4}= 0.4 g/g and **x = 11**.*

Figure 22 plots pressure and internal temperature in function of time for the experiments performed with a hydration factor of 11. The results obtained are similar and, when compared with studies carried out at uncontrolled room temperature, there is an increase in the hydrogen generation rates and a decrease of the induction time.

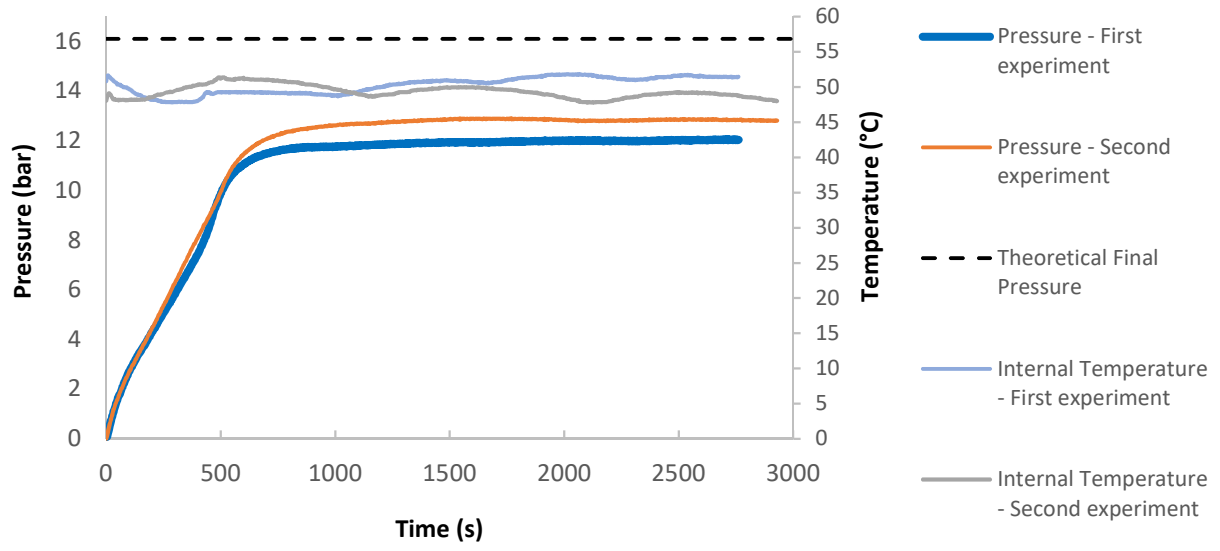

Figure 23 - Chart of hydrogen generation for an alkali free hydrolysis of sodium borohydride, at 50 ± 5 ºC, to study the influence of the temperature with the following conditions: m_{NaBH_4} *= 0.048 g,* m_{Cat}/m_{NaBH_4} *= 0.4 g/g and* ***x = 2****.*

The results of the experiments carried out at 50 ºC and with an *x* of 2 are displayed in Figure 23. Despite the second experiment present a higher final pressure, and consequently a higher yield, the results are quite similar between both experiments. Nevertheless, it was observed again that the increasing of the temperature causes an increase of the hydrogen generation rates.

Finally, Table 8 presents a summary of the experiments performed and the results obtained for all the experiments mentioned before. The experiments carried out at 50 ºC were useful to study the performance of the catalyst and it is evident that the experiments with higher temperature had a lower induction time and a higher *HGR*. Nevertheless, the use of high temperature is not profitable, since it is necessary to use energy to increase the reaction's medium temperature, and the aim of this technology is to produce energy without expend energy. Moreover, it was not performed any experiment with a hydration factor of 0, at a temperature of 50 ºC, given the duration of the experiment and the results obtained previously.

Nunes *et al.* [60] reported a yield of 90.40 % and a *HGR* of 980 $mL_{H_2} min^{-1} g_{Cat}^{-1}$ for an experiment with a hydration factor of 16, at uncontrolled room temperature, which is an intermediary value between the two experiments performed in the present work. Nevertheless, the *HGR* reported was considerably higher. The hydrogen generation rate obtained was closer to the 570 $mL_{H_2} min^{-1} g_{Cat}^{-1}$ described by Crisafulli *et al.* [57]. Although the higher *HGR* obtained was for an *x* equal to 16, at uncontrolled room temperature, the excess of water enhanced borate solubility which lead to a decrease of volumetric and gravimetric storage density.

Table 8 - Results of the experiments performed of the sodium borohydride hydrolysis with different hydration factors.

x	*Temperature (ºC)*	*η (%)*	Induction time (s)	*dP/dt (bar s^{-1})*	*HGR ($mL_{H_2} min^{-1} g_{Cat}^{-1}$)*	*GHSC (wt%)*	*VHSC (kg m^{-3})*
16	24	87.98	28.64	1.52×10^{-2}	387	1.72	19.01
	25	93.06	26.14	1.73×10^{-2}	429	1.83	20.18
	51	90.73	4.72	1.97×10^{-1}	4 753	1.78	19.66
	48	89.53	7.55	1.81×10^{-1}	4 389	1.76	19.38
11	25	91.70	29.39	1.81×10^{-2}	355	2.32	25.79
	24	91.68	29.85	1.71×10^{-2}	337	2.32	25.79
	50	88.41	5.31	2.34×10^{-1}	4 375	2.23	24.84
	49	91.80	5.70	3.09×10^{-1}	5 775	2.32	25.83
2	23	87.43	100.44	1.90×10^{-3}	51	5.24	58.27
	22	88.36	85.63	1.90×10^{-3}	51	5.30	58.93
	48	80.72	13.84	1.57×10^{-2}	385	4.85	53.89
	47	86.29	11.87	1.82×10^{-2}	448	5.18	57.64
0	22	81.78	126.56	9.00×10^{-4}	24	6.93	80.75
				3.69×10^{-9}	0.27		
	24	71.84	163.75	1.00×10^{-3}	25	6.21	73.01
				1.84×10^{-9}	0.12		

4.3.4 Impact of the use of 50 ºC in the catalyst

After the use of the unsupported catalyst at 50ºC it was questioned if it would have significant impact in the performance of the catalyst. Thus, an experiment with a hydration factor of 16 was carried out to assess the performance of the catalyst and the results obtained are displayed in Figure 24.

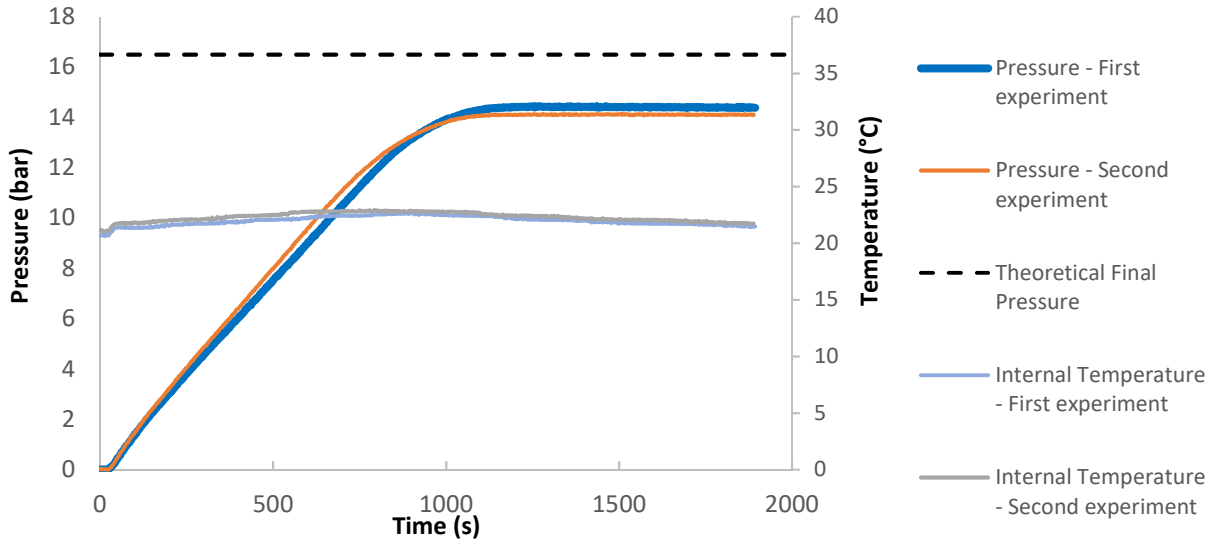

Figure 24 - Chart of hydrogen generation for a classic hydrolysis of sodium borohydride, at uncontrolled room temperature, to study the impact of the use of a temperature of 50 ºC in the catalyst with the following conditions: m_{NaBH_4} *= 0.052 g,* m_{Cat}/m_{NaBH_4} *= 0.4 g/g and* ***x = 16****.*

Comparing the results with the previously presented in Figure 17 – performed at the same conditions - no significant differences were found, with the exception of the induction time that almost doubled, from around 26 or 28 s to 51 or 53 s, as it is observable in Table 9.

Table 9 - Results of the experiment performed at uncontrolled room temperature with the catalyst reused after studies carried out at 50 ºC.

x	*Temperature (ºC)*	*η (%)*	Induction time (s)	*dP/dt (bar* s^{-1}*)*	*HGR* ($mL_{H_2} min^{-1} g_{Cat}^{-1}$)	*GHSC (wt%)*	*VHSC (kg* m^{-3}*)*
16 before	24	87.98	28.64	1.52×10^{-2}	387	1.72	19.01
	25	93.06	26.14	1.73×10^{-2}	429	1.83	20.18
16 after	22	93.70	53.34	1.49×10^{-2}	384	1.84	20.35
	22	91.42	51.44	1.58×10^{-2}	407	1.80	19.82

4.4 Study of the supported catalyst

The performance of the supported catalysts - previously reported in Table 6 presented in Chapter 3 – in the hydrolysis of $NaBH_4$ - was studied. The different catalysts were denominated by ESPRU 1, ESPRU 2 and ESPRU 3, and presented the concentrations of 2.04, 0.95 and 0.44 mg of catalyst, respectively. The supported catalyst has the advantage of being easier to handle and clean (both the catalyst and the reactor) than the unsupported catalyst.

The main goal of use a supported catalyst is to achieve the same reaction rates as with the unsupported catalysts however, with a low amount of reactants, since the porosity of the supported catalyst enhances the contact between them and the active area of the catalyst. Therefore, the catalyst/$NaBH_4$ mass ratio was reduced to a quarter of the used with the unsupported catalyst, i.e., 0.1 g/g, for the experiments with ESPRU 1 and ESPRU 2, in order to use a substantial minimum amount of reactants to perform the hydrolysis reaction. The results obtained were quite interesting with similar hydrogen generation rates and, since ESPRU 2 presented less amount of catalyst, comparative studies with the same amount of $NaBH_4$ between the hydrolysis with ESPRU 2 and ESPRU 3 were performed. The results of this studies are shown in Figures 25 to 30 and summarised in Table 10.

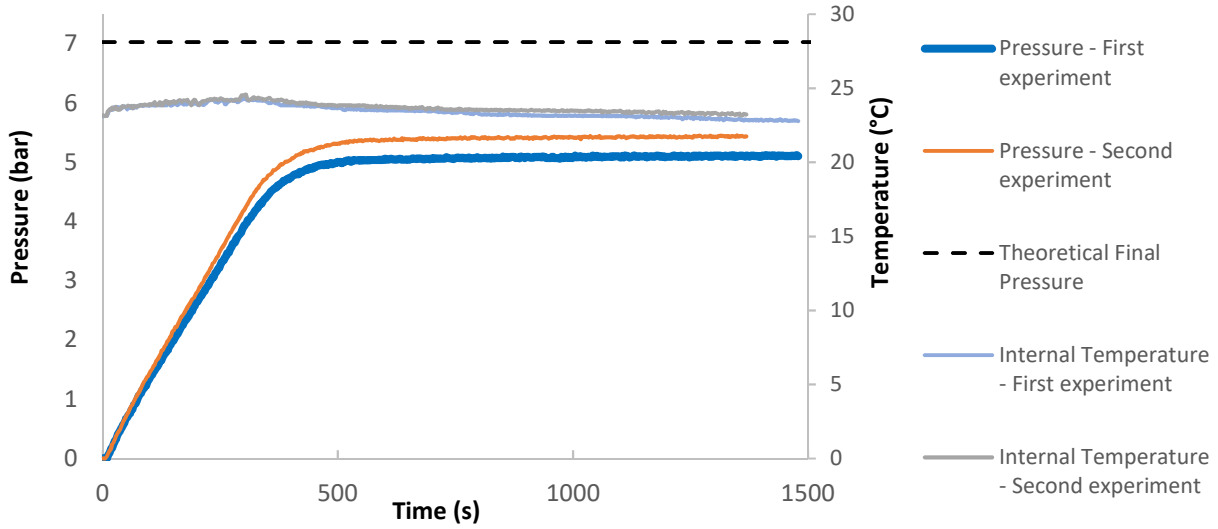

*Figure 25 - Chart of hydrogen generation for a classic hydrolysis of sodium borohydride using the **ESPRU 1**, at uncontrolled room temperature, to study the influence of the hydration factor with the following conditions: $m_{catalyst\ in\ the\ support}$ = 2.04 mg, m_{NaBH_4} = 0.020 g and 0.021 g, respectively, m_{Cat}/m_{NaBH_4} = 0.1 g/g and **x = 16**.*

Figure 25 illustrates the results obtained with ESPRU 1 and an *x* of 16. The behaviour of the internal temperature was similar to the other experiments and had a slight increase during the hydrogen production. The *HGRs* values obtained were considerable higher than the obtained for the unsupported catalyst, 3 231 and 3 476 $mL_{H_2}min^{-1}\ g_{Cat}^{-1}$, and the reaction yields were similar, which is advantageous since the catalyst/$NaBH_4$ mass ratio used was four times lower than the used with the unsupported catalyst.

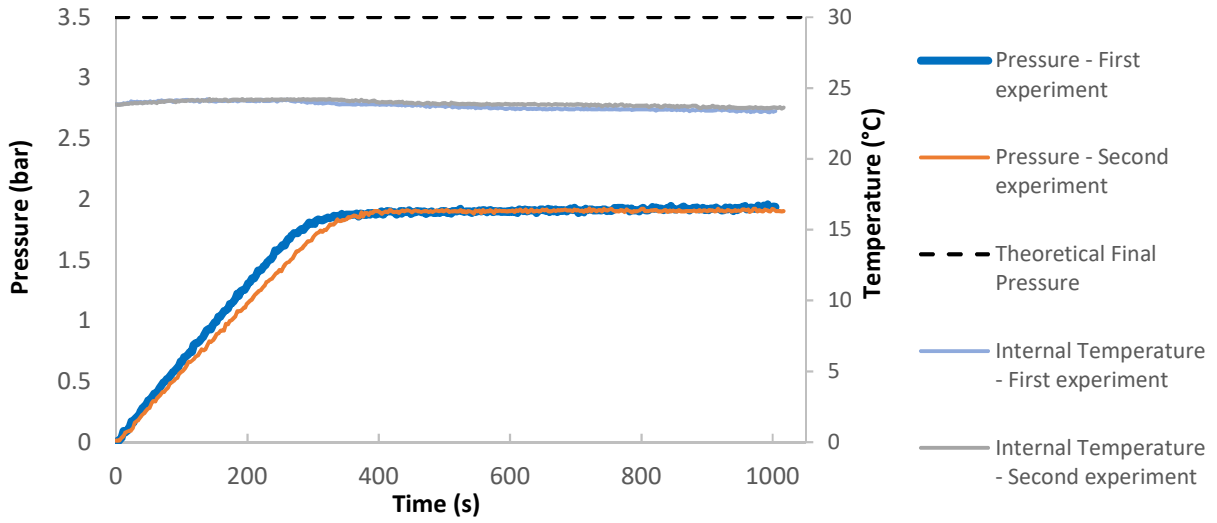

*Figure 26 - Chart of hydrogen generation for a classic hydrolysis of sodium borohydride using the **ESPRU 2**, at uncontrolled room temperature, to study the influence of the hydration factor with the following conditions: $m_{catalyst\ in\ the\ support}$ = 0.95 mg, m_{NaBH_4} = 0.008 g, m_{Cat}/m_{NaBH_4} = 0.1 g/g, respectively, and **x = 16**.*

The results obtained for the experiments with ESPRU 2 and an *x* equal to 16 are shown in Figure 26. Both experiments presented similar results and although the reaction yields were lower than the obtained with ESPRU 1, 83.80 and 83.47 %, it is noteworthy the theoretical final pressure value of 3.50 bar which might misleadingly enhance the difference between the theoretical and experimental pressure values. Moreover, the hydrogen generation rates (3 407 and 3 018 $mL_{H_2}min^{-1}\ g_{Cat}^{-1}$) were similar to the obtained with ESPRU 1, which presents an advantage since ESPRU 2 contains less amount of catalyst, i.e., is cheaper.

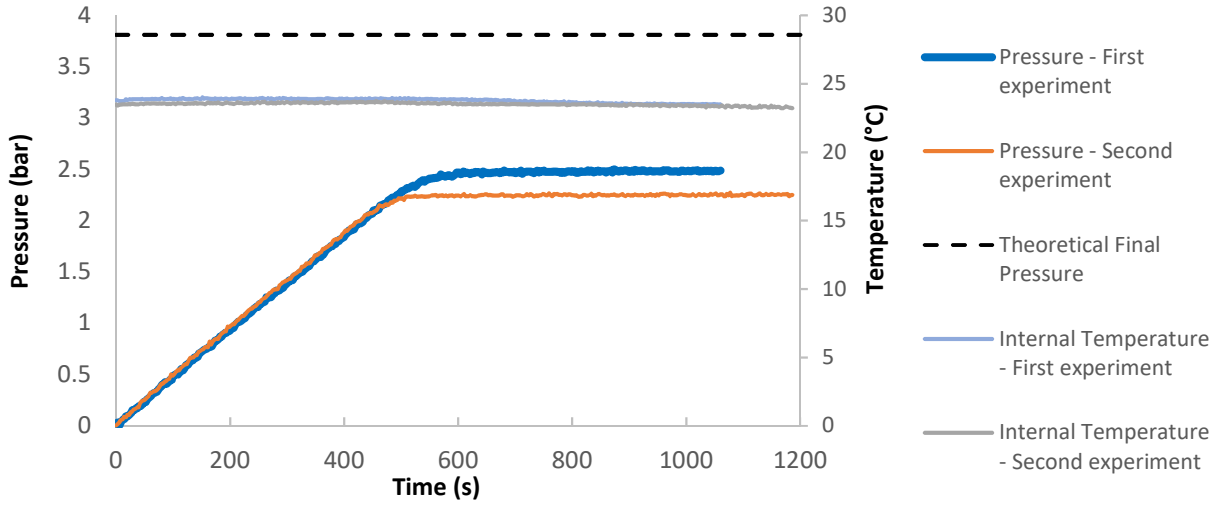

*Figure 27 - Chart of hydrogen generation for a classic hydrolysis of sodium borohydride using the **ESPRU 3**, at uncontrolled room temperature, to study the influence of the hydration factor with the following conditions: $m_{catalyst\ in\ the\ support}$ = 0.44 mg, m_{NaBH_4} = 0.009 g, m_{Cat}/m_{NaBH_4} = 0.05 g/g and **x = 16**.*

Figure 27 shows the plot with the results obtained with ESPRU 3 and a hydration factor of 16. Although the linear region slope of both experiments were similar, the first experiment had a final pressure higher than the second one, leading to a difference in the yields from 91.23 % to

86.09 %. The achieved hydrogen generation rates of 5 328 and 5 463 $mL_{H_2} min^{-1} g_{Cat}^{-1}$ stand out, since they are higher than the rates achieved from the experiments with the unsupported catalyst at 50ºC, obtained with a higher catalyst/$NaBH_4$ mass ratio.

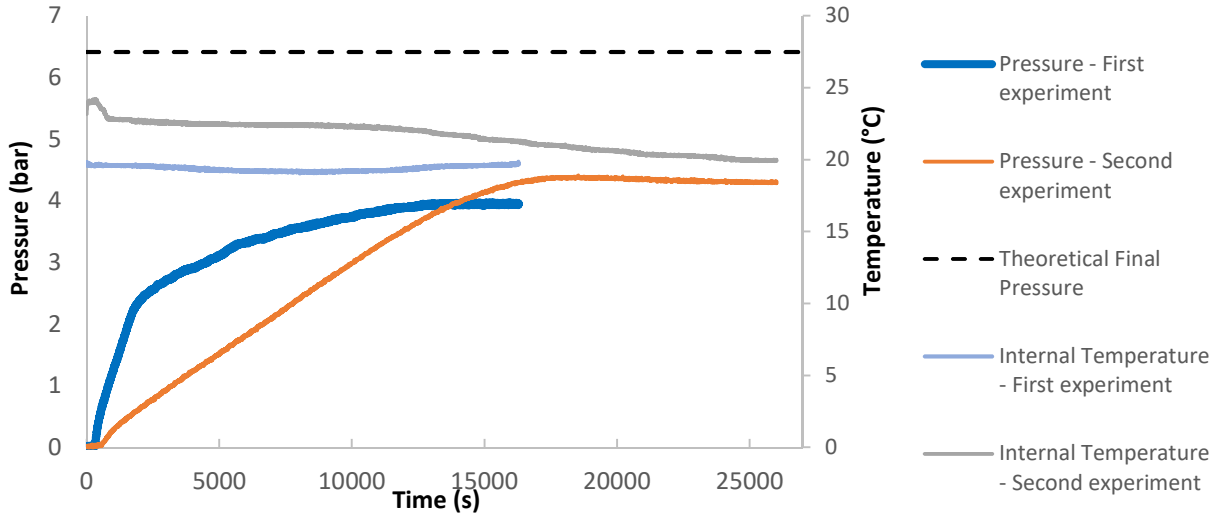

*Figure 28 - Chart of hydrogen generation for an alkali free hydrolysis of sodium borohydride using the **ESPRU 1**, at uncontrolled room temperature, to study the influence of the hydration factor with the following conditions: $m_{catalyst\ in\ the\ support}$ = 2.04 mg, m_{NaBH_4} = 0.018 g and 0.019 g, respectively, m_{Cat}/m_{NaBH_4} = 0.1 g/g and **x = 2**.*

Besides the experiments with a hydration factor of 16, studies with an *x* of 2 were also performed. The results using the catalyst ESPRU 1 are plotted in Figure 28 and, as can be seen the two experiments were very different. Although the first experiment showed a lower yield, the linear region slope was higher and, consequently, presented a higher hydrogen generation rate. Moreover, after the first experiment (third reutilisation) it was observed a deterioration of the coating, which is a possible explanation for the differences observed in the experiments.

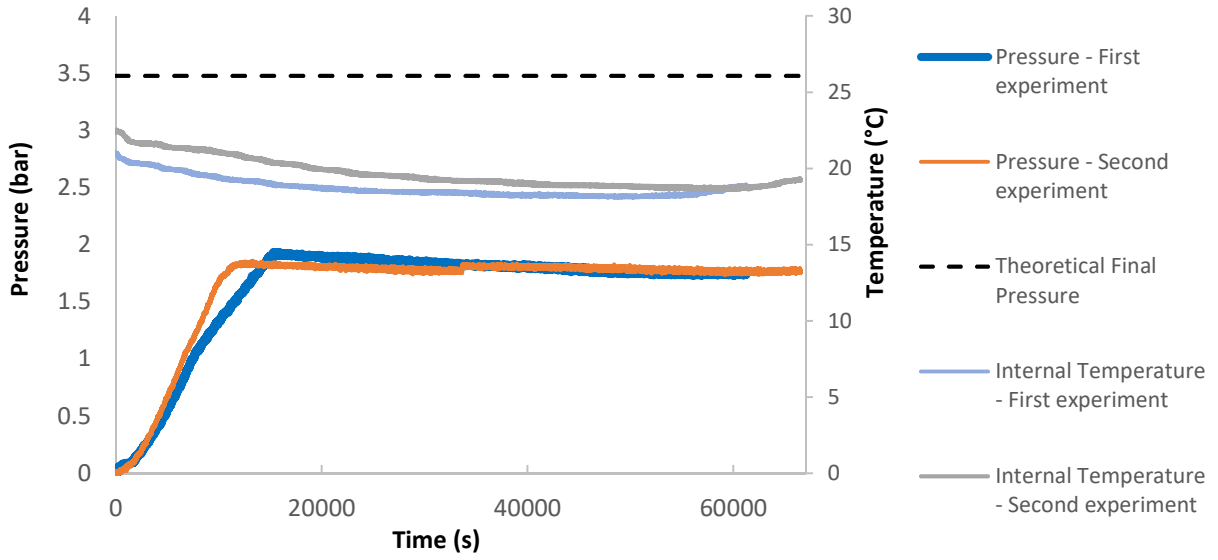

*Figure 29 - Chart of hydrogen generation for an alkali free hydrolysis of sodium borohydride using the **ESPRU 2**, at uncontrolled room temperature, to study the influence of the hydration factor with the following conditions: $m_{catalyst\ in\ the\ support}$ = 0.95 mg, m_{NaBH_4} = 0.008 g and 0.009 g, respectively, m_{Cat}/m_{NaBH_4}= 0.1 g/g and **x = 2**.*

Figure 29 displays the results for the experiments performed with an *x* of 2, using ESPRU 2. This supported catalyst showed a different behaviour when compared with the other supported catalysts, since the pressure plot presented a small peak right before achieved the final plateau. Moreover, temperature presented a significant decrease which can be explained to the fact that both experiments were performed overnight, when it is usual to occur a slight decrease of temperature. In this study, reaction yields of 80.07 and 79.25 % were obtained and the *HGR* was 112 $mL_{H_2} min^{-1} g_{Cat}^{-1}$ for both experiments. The yields were slightly lower than the values reported in Table 8 for the experiments performed in the same conditions with the unsupported catalyst however, the *HGR* obtained was higher.

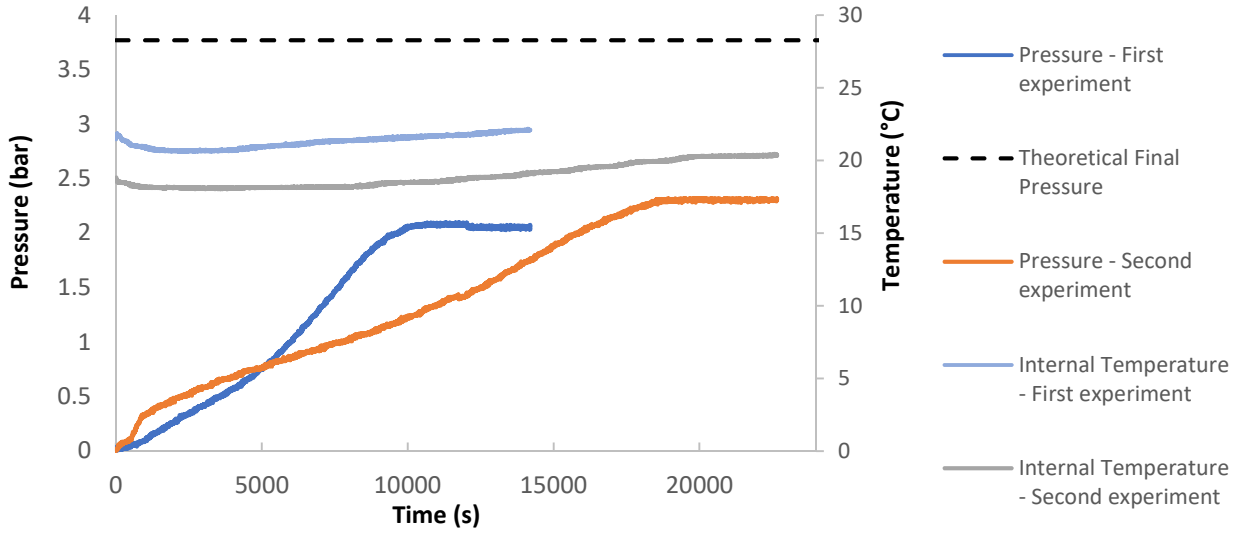

*Figure 30 - Chart of hydrogen generation for an alkali free hydrolysis of sodium borohydride using the **ESPRU 3**, at uncontrolled room temperature, to study the influence of the hydration factor with the following conditions: $m_{catalyst\ in\ the\ support}$ = 0.44 mg, m_{NaBH_4} = 0.009 g, m_{Cat}/m_{NaBH_4}= 0.05 g/g and **x = 2**.*

The results obtained using ESPRU 3 are presented in Figure 30 and, as it happened for the plot with ESPRU 1, the experiments are not similar. Once again, these results can be explained with the deterioration of the coating observed. Moreover, since it was used a small amount of reactants and the catalyst coating was not uniform (as observed in SEM analysis), it is possibly that the reactants may have difficulty to reach the catalyst in all the active area and, consequently, have a negative impact in the catalysts performance. However, the hydrogen generation rate obtained in the first experiment was the highest with the hydration factor of 2 (360 $mL_{H_2} min^{-1} g_{Cat}^{-1}$), which was remarkable, since the catalyst/$NaBH_4$ mass ratio was halved.

Furthermore, aiming to achieved high *HGR*s, experiments with a hydration factor of 2 and the approximate $NaBH_4$ amount of 0.05 g, were performed. Nevertheless, the experiments were not replicated, since a quickly deterioration of the coating in the supported catalysts was observed, as it is presented in Figure C.1 of Appendix C, and, consequently, it was not possible to ensure the same conditions. The results obtained are presented in Figures 31 to 33.

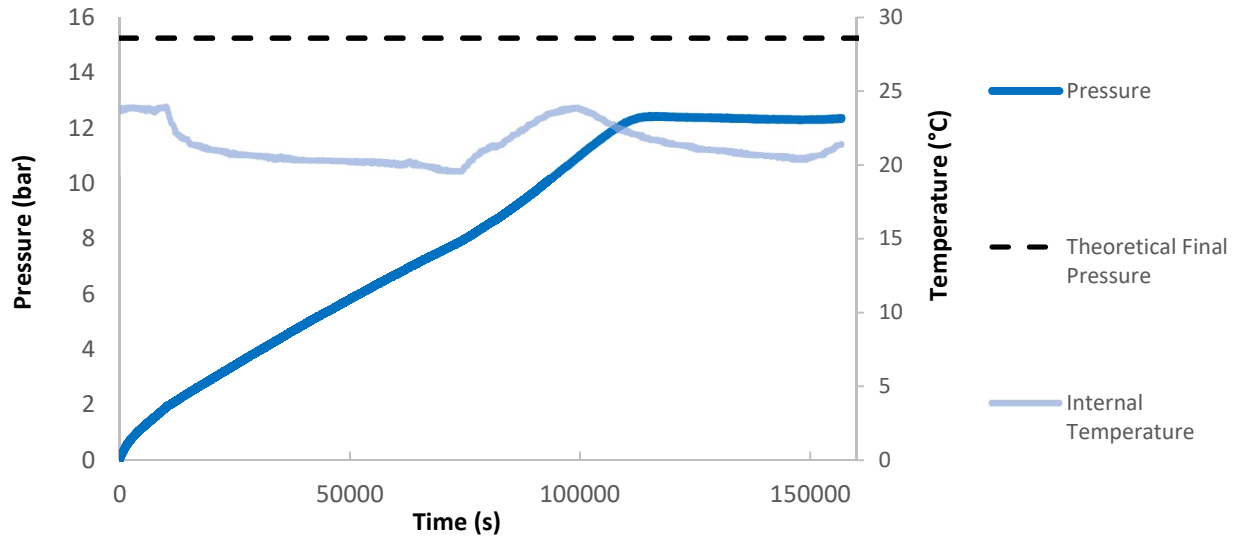

*Figure 31 - Chart of hydrogen generation for an alkali free hydrolysis of sodium borohydride using the **ESPRU 1**, at uncontrolled room temperature, to study the influence of the hydration factor with the following conditions: $m_{catalyst\ in\ the\ support}$ = 2.04 mg, m_{NaBH_4} = 0.048 g, m_{Cat}/m_{NaBH_4} = 0.04 g/g and **x = 2**.*

Figure 31 present the results obtained with the ESPRU 1 catalyst with an *x* of 2 and a catalyst/$NaBH_4$ mass ratio of 0.04 g/g, which meant it was used an amount of $NaBH_4$ of around 0.05 g, similar to the value used in the experiments carried out with the unsupported catalyst. The temperature varied throughout the experiment, since the temperature was changeable during the day and night. Comparing with the results presented in Figure 28, the study shows an increase of the reaction yield and it was similar to the yield obtained with ESPRU 3 and the same catalyst/$NaBH_4$ mass ratio. Moreover, a decrease of the *HGR* can be observed, which was expected since the catalyst/$NaBH_4$ mass ratio was decreased.

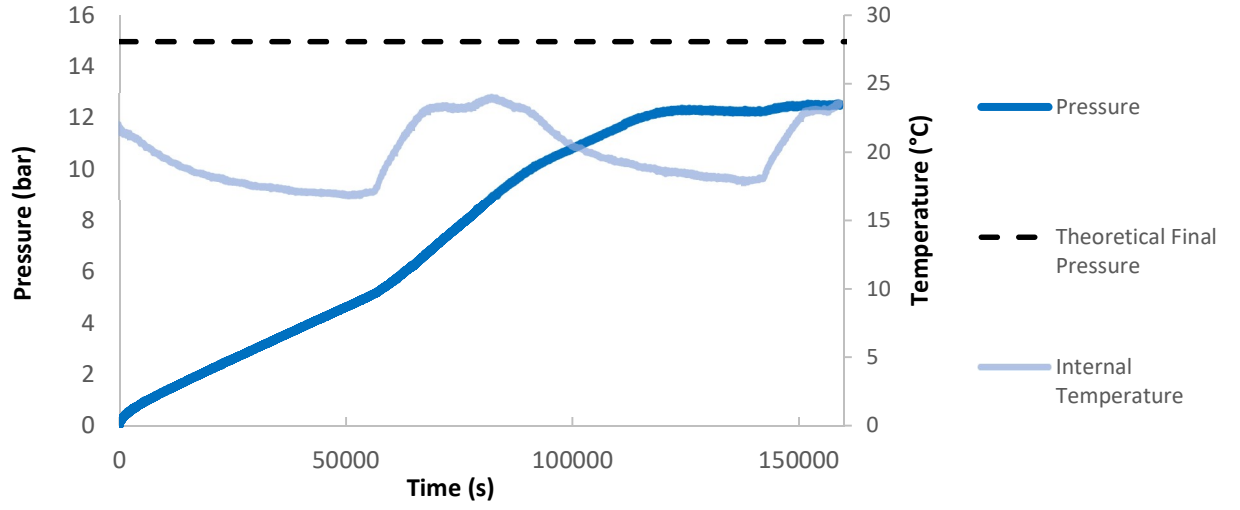

*Figure 32 - Chart of hydrogen generation for an alkali free hydrolysis of sodium borohydride, at uncontrolled room temperature, using the **ESPRU 2**, to study the influence of the hydration factor with the following conditions: $m_{catalyst\ in\ the\ support}$ = 0.95 mg, m_{NaBH_4} = 0.048 g, m_{Cat}/m_{NaBH_4} = 0.02 g/g and **x = 2**.*

Through the results plotted in Figure 32, with ESPRU 2, a temperature variation can be observable, once again due to the experiment lasted about two days. Therefore, this variation

had a slight influence in the *HGR* since it increased with the increase of temperature, thus it was considered two distinct linear regions (one with a higher slope value than the other). Moreover, the amount of $NaBH_4$ used was the same of the previous experiment and, consequently, the catalyst/$NaBH_4$ mass ratio was 0.02 g/g. Comparing the results with the presented in Figure 29, a higher yield was achieved and the *HGR* value was lower.

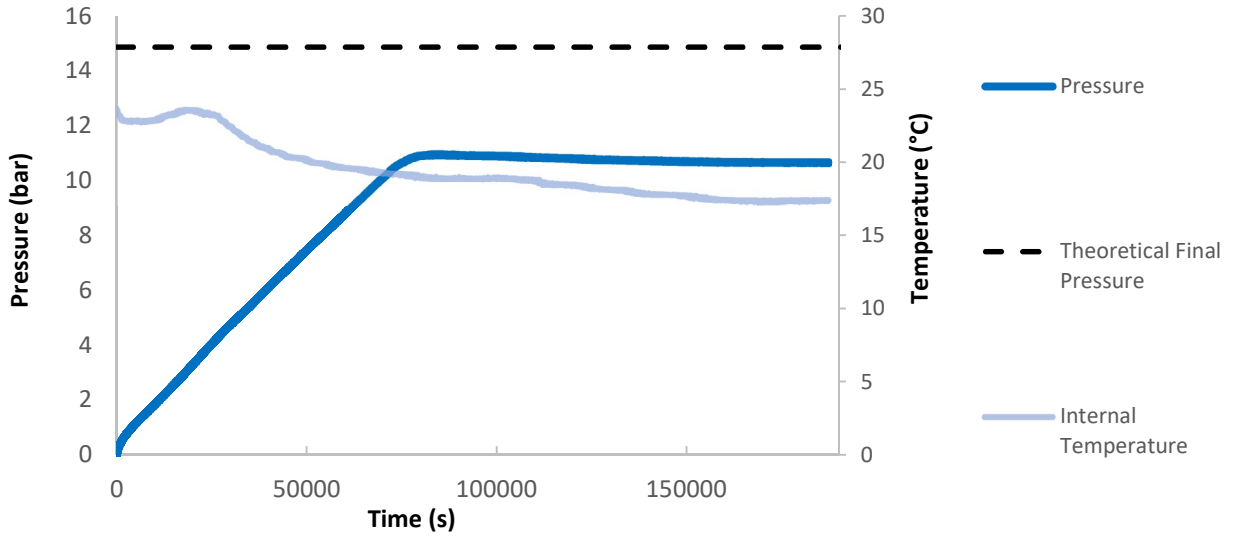

*Figure 33 - Chart of hydrogen generation for an alkali free hydrolysis of sodium borohydride using the **ESPRU 3**, at uncontrolled room temperature, to study the influence of the hydration factor with the following conditions: $m_{catalyst\ in\ the\ support}$ = 0.44 mg, m_{NaBH_4} = 0.048 g, m_{Cat}/m_{NaBH_4} = 0.01 g/g and **x = 2**.*

The results of the last experiment performed with ESPRU 3 are represented in Figure 33 and, comparing to Figure 30, the *HGR* obtained was similar to the one obtained in the second experiment and the reaction yield was lower. Nevertheless, the catalyst/$NaBH_4$ mass ratio was considerably lower (since it was kept constant the amount of $NaBH_4$).

The results obtained for all the experiments performed with the supported catalysts are summarised in Table 10. The higher *HGR* achieved was 5 463 $mL_{H_2}min^{-1}\ g_{Cat}^{-1}$ using ESPRU 3 catalyst and an *x* of 16, which was substantially higher than the 2 400 $mL_{H_2}min^{-1}\ g_{Cat}^{-1}$ obtained by Krishnan *et al.* [42] using a catalyst of Pt/Ru-$LiCoO_2$ dispersed on a Ni mesh, shown previously in Table 4 of Chapter 2. The induction times in the experiments carried out with a hydration factor of 16 were comparable to the obtained for the unsupported catalyst (in Table 8) however, the yields were lower and the *HGRs* values were higher.

The lower *HGR* was achieved for the experiments carried out with an *x* of 2, nevertheless, these values are comparable with the values reported by Huang *et al.* [56] (*HGR* of 68.2 $mL_{H_2}min^{-1}\ g_{Cat}^{-1}$) for a Ru composite catalyst supported on alumina. Comparing with the results obtained with the unsupported catalyst, despite the induction times were sustainable higher, the *HGRs* were also higher.

Therefore, it can be concluded that the supported catalysts of Ru on Ni foam are easier to handle and clean and can be successfully used in the hydrolysis of $NaBH_4$. Although the *HGRs* for an *x* of 2 were slow, with an *x* equal to 16 the supported catalysts presented a better behaviour than the unsupported catalyst at 50 ºC. These results stand out since the issue related with energy consumption may be overcome. Nevertheless, these catalysts showed a quick degradation, as it is possible to observe in Figure C.1 of Appendix C, which are major disadvantages for a real application.

Table 10 - Results of the experiments using the supported catalyst and performed with different hydration factors, at uncontrolled room temperature.

x	*Catalyst ESPRU*	catalyst/$NaBH_4$ *(g/g)*	*Temperature (ºC)*	*η (%)*	Induction time (s)	*dP/dt (bar s^{-1})*	*HGR ($mL_{H_2} min^{-1} g^{-1}_{Cat}$)*	*GHSC (wt%)*	*VHSC ($kg\ m^{-3}$)*
16	1	0.1	23	89.40	38.49	1.27×10^{-2}	3 231	1.46	9.15
		0.1	24	89.23	37.11	1.37×10^{-2}	3 476	1.47	9.43
	2	0.1	24	83.80	74.17	6.20×10^{-3}	3 407	1.02	4.66
		0.1	25	83.47	86.71	5.50×10^{-3}	3 018	1.01	4.62
	3	0.05	24	91.23	104.09	4.50×10^{-3}	5 328	1.20	5.69
		0.05	24	86.09	96.32	4.60×10^{-3}	5 463	1.10	5.20
2	1	0.1	21	78.26	484.92	1.30×10^{-3}	338	2.84	10.95
						2.00×10^{-4}	52		
		0.1	22	82.21	1581.13	3.00×10^{-4}	78	3.04	11.84
	2	0.1	20	80.07	4643.72	2.00×10^{-4}	112	1.76	5.34
		0.1	21	79.25	4031.39	2.00×10^{-4}	112	1.69	5.32
	3	0.05	22	81.24	3439.26	3.00×10^{-4}	360	1.90	5.98
		0.05	20	88.35	2124.05	9.00×10^{-5}	109	2.17	6.78
	1	0.04	23	87.47	1230.57	9.00×10^{-5}	23	4.69	25.47
	2	0.02	20	90.22	1673.07	8.00×10^{-5}	45	4.80	25.92
						1.00×10^{-4}	57		
	3	0.01	21	78.55	1180.18	1.00×10^{-4}	123	4.14	49.23

5. Conclusions

The aim of this work was to study the performance of two types of Ni-Ru catalysts – supported and unsupported - applied to the hydrolysis of sodium borohydride for hydrogen generation. In order to characterize the catalysts, they were analysed through SEM, EDX and XRD techniques. In the unsupported catalysts analysed, both non-used and reused, it was found nickel, ruthenium, oxygen and carbon elements. Moreover, any significant differences were not found between the non-used catalyst and the reused once, which indicates that the experimental procedure and the washing/recycle technique were adequate. In the supported catalysts, XRD analysis was in agreement with the elements found in the EDX analysis - nickel (in the form of oxide and metal), ruthenium and oxygen. Furthermore, together with SEM analysis, it was possible to observe that the catalyst was supported on Ni foam.

Several experiments were performed with the unsupported catalyst to assess the influence of the hydration factor and of the temperature in the performance of the catalyst. This catalyst had an analogous behaviour to the reported by Nunes [30] and Nunes *et al*. [60], which was expected since it was similar to the previous catalyst used. According to the literature, the yield and the hydrogen generation rate increase with the increase of the hydration factor. However, the gravimetric and volumetric storage capacities decrease, which was verified in this work.

The highest hydrogen generation rate obtained was 5 775 $mL_{H_2} min^{-1} g_{Cat}^{-1}$ for the experiment carried out with the unsupported catalyst, a hydration factor of 11 and a temperature of 49 ºC. The hydrogen generation rates of the experiments performed at 50 ºC were satisfactory, nevertheless these conditions are not profitable since it is necessary to use energy to increase the reaction's medium temperature. Additionally, it was concluded that the experiments carried out at 50 ºC did not influence the behaviour of the catalyst in further experiments.

Likewise, the influence of the catalyst/$NaBH_4$ mass ratio and of the amount of sodium borohydride were studied in the experiments carried out with the supported catalysts. Yields between 78.26 and 91.23 % were achieved, which were satisfactory and closer to the ones obtained with the unsupported catalyst. The higher hydrogen generation rate was 5 463 $mL_{H_2} min^{-1} g_{Cat}^{-1}$ performed with the ESPRU 3, at uncontrolled room temperature, a hydration factor of 16 and a catalyst/$NaBH_4$ mass ratio of 0.05 g/g. This hydrogen generation rate is obtained with a low amount of catalyst present in the foam (0.44 mg), which is advantageous and makes it more profitable for real applications since it makes the catalyst cheaper (it is noteworthy that one of the biggest disadvantage of the noble metal catalysts is its cost).

Comparing the results obtained from ESPRU 3 with the Ni-Ru unsupported catalyst, the hydrogen generation rates obtained with the supported catalyst were similar to the obtained with the unsupported catalyst at 50 ºC. Moreover, the hydrogen generation rate obtained in the experiment with a hydration factor of 16 was higher, as it is shown in Figure 34. Therefore, it possible to conclude that the use of the supported catalysts is an advantage since it was obtained similar results without spend an external source of energy to increase the temperature of the reaction's medium.

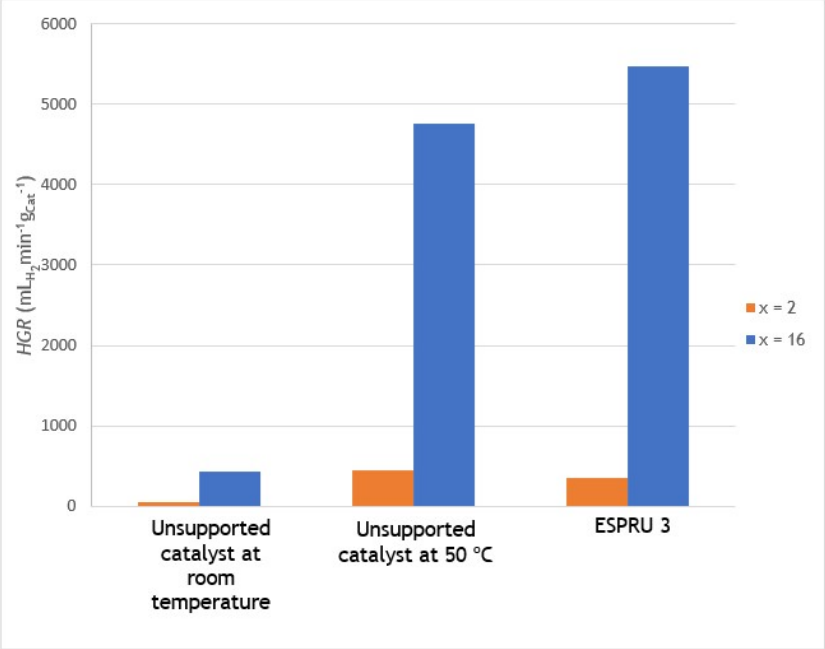

Figure 34 – Chart with the comparison between the results obtained for the unsupported catalyst and the supported catalyst ESPRU 3.

In summary, the supported catalysts (studied for the first time within the research group) represent a biggest advantage in the feasibility for portable applications, owing to the fact that both the reactor and the catalyst were easier to handle and clean, when compared to the unsupported catalyst. Moreover, the hydrogen generation rates obtained with a hydration factor of 16 confirm the possibility of using these supported catalysts in portable applications. It is noteworthy that the main disadvantage of using the supported catalysts was the obvious degradation after only three reutilisations. Moreover, the use of small amounts of water can also influence the reaction rates and, consequently, be a disadvantage, since the deposition of catalyst in the support was not uniform which is a difficulty to the access of the reactants to the active area of the catalyst.

6. Assessment of the work done

This chapter presents a brief evaluation of this work, including the objectives achieved, the limitations noted, suggestions for future work and a final appreciation.

6.1 Achieved goals

The development of a profitable technology to produce hydrogen through sodium borohydride hydrolysis is fundamental to the development of a hydrogen economy. The research of a suitable catalyst has the major role, in order to improve the reaction rates and the storage densities and, consequently, to fulfil the requirements of U.S. DOE for hydrogen storage systems.

This work had the main goal, which was accomplished, of studying an unsupported catalyst of Ni-Ru and three identical supported catalysts - with different concentrations of Ru coating in the support – and, compare the results between them and with the values reported in the literature.

The unsupported catalyst presented similar results to the unsupported catalyst previously studied in the laboratory [1], [33], [60], [64], i.e., it presented satisfactory results for a temperature at 50 ºC, nevertheless, at room temperature, the reaction rates are low.

The supported catalyst shown to be easier to handle and clean (either the catalyst and the reactor), which is a major advantage for the portable applications. Furthermore, with a hydration factor of 16, the reaction rates achieved were higher than the obtained with the unsupported catalyst, at uncontrolled room temperature, and comparable to the obtained with the unsupported catalyst and at 50 ºC. Since it was used a small amount of catalyst and a lower catalyst/$NaBH_4$ mass ratio, the results obtained for the supported catalysts represent a significant improvement in the reaction rates and increases the feasibility for portable applications. However, the ideal is to develop a catalyst that improve the hydrolysis reaction in order to achieve, with a hydration factor of 2, the same rates obtained with a hydration factor of 16.

6.2 Limitations and future work

The hydrogen generation through chemical hydrides will be a common energy carrier, mainly in remote locations without grid. However, it is necessary to overcome some issues such as the low gravimetric and volumetric storage capacities. To do that, the hydration factor should be stablished between 0 and 2, nevertheless, with that conditions, the hydrogen generation rate is too slow.

The results obtained in this work for the supported catalysts and with an *x* of 2 should be repeated with new supported catalysts, since the performance of the ones tested in this work was already decreasing. Moreover, the supported catalysts were only reused 5 times, therefore it should be studied a possibility to synthesise a more resistant catalyst, i.e., a catalyst coating with a stronger adhesion to the support, in order to improve its durability and capability to be reused.

Finally, the kinetics for the sodium borohydride hydrolysis should also be studied, in order to develop a kinetic model that correctly describes the reaction behaves in function of concentration of reactants, pressure and temperature in the mini-egg shaped reactor.

6.3 Final appreciation

From a personal point of view, I must tell that my experience was beyond the expected. It was a privilege to develop my thesis in a subject that is so meaningful to me and, at the same time, to know so interesting people.

It is quite rewarding to think that in somehow, I gave my contribute to the research and improvement of a hydrogen generation system, that one day will be one of the bases for a new energetic economy, and I will certainly follow the new findings from CEFT. Furthermore, it was a challenge to write this thesis in English however, I think it was an achievement.

7. References

[1] A. M. F. R. Pinto, M. J. F. Ferreira, V. R. Fernandes, and C. M. Rangel, "Durability and reutilization capabilities of a Ni-Ru catalyst for the hydrolysis of sodium borohydride in batch reactors," *Catal. Today*, vol. 170, no. 1, pp. 40–49, 2011.

[2] J. Rifkin, *The hydrogen economy: the creation of the wordwide energy web and the redistribution of power on earth*, First. TarcherPerigee, 2003.

[3] F. M. Dos Santos and F. A. Dos Santos, "O combustível 'hidrogénio,'" *Milen. on.line*, vol. 31, pp. 252–270, 2005.

[4] M. J. F. Ferreira, L. Gales, V. R. Fernandes, C. M. Rangel, and A. M. F. R. Pinto, "Alkali free hydrolysis of sodium borohydride for hydrogen generation under pressure," *Int. J. Hydrogen Energy*, vol. 35, no. 18, pp. 9869–9878, 2010.

[5] U. B. Demirci, O. Akdim, J. Andrieux, J. Hannauer, R. Chamoun, and P. Miele, "Sodium borohydride hydrolysis as hydrogen generator: Issues, state of the art and applicability upstream from a fuel cell," *Fuel Cells*, vol. 10, no. 3, pp. 335–350, 2010.

[6] S. C. Amendola, S. S. Goldman, M. Janjua, N. Sprencer, M. Kelly, P. Petillo, and M. Binder , "A Safe, portable, hydrogen gas generator using aqueous borohydride solution and Ru catalyst," *Int. J. Hydrogen Energy*, vol. 25, no. 10, pp. 969–975, 2000.

[7] H. I. Schlesinger, H. C. Brown, A. E. Finholt, R. Gilbreath, H. R. Hoekstra, and E. K. Hyde, "Sodium Borohydride , its hydrolysis and its use as a reducing agent and in the generation of hydrogen," *J. Am. Chem. Soc*, vol. 75, no. 1, pp. 215–219, 1953.

[8] B. H. Liu and Z. P. Li, "A review: Hydrogen generation from borohydride hydrolysis reaction," *J. Power Sources*, vol. 187, no. 2, pp. 527–534, 2009.

[9] H. C. Brown and C. A. Brown, "New, highly active metal catalysts for the hydrolysis of borohydride," *J. Am. Chem. Soc*, vol. 84, pp. 1493–1494, 1962.

[10] U. B. Demirci, "The hydrogen cycle with the hydrolysis of sodium borohydride: A statistical approach for highlighting the scientific/technical issues to prioritize in the field," *Int. J. Hydrogen Energy*, vol. 40, no. 6, pp. 2673–2691, 2015.

[11] U. B. Demirci and F. Garin, "Ru-based bimetallic alloys for hydrogen generation by hydrolysis of sodium tetrahydroborate," *J. Alloys Compd.*, vol. 463, no. 1–2, pp. 107–111, 2008.

[12] J. Kim, K. Kim, Y. Kang, H. Kim, M. Song, Y. Lee, and J. Lee, "Study on degradation of filamentary Ni catalyst on hydrolysis of sodium borohydride," *J. Alloys Compd.*, vol. 379, no. 1–2, pp. 222–227, 2004.

[13] Q. Zhang, G. Smith, Y. Wu, and R. Mohring, "Catalytic hydrolysis of sodium borohydride in an auto-thermal fixed-bed reactor," *Int. J. Hydrogen Energy*, vol. 31, no. 7, pp. 961–965, 2006.

[14] R. Peña-Alonso, A. Sicurelli, E. Callone, G. Carturan, and R. Raj, "A picoscale catalyst for hydrogen generation from NaBH4 for fuel cells," *J. Power Sources*, vol. 165, no. 1, pp. 315–323, 2007.

[15] E. Keçeli and S. Özkar, "Ruthenium(III) acetylacetonate: A homogeneous catalyst in the hydrolysis of sodium borohydride," *J. Mol. Catal. A Chem.*, vol. 286, no. 1–2, pp. 87–91, 2008.

[16] S. C. Amendola, S. L. Sharp-Goldman, M. S. Janjua, M. T. Kelly, P. J. Petillo, and M. Binder, "An ultrasafe hydrogen generator: Aqueous, alkaline borohydride solutions and Ru catalyst," *J. Power Sources*, vol. 85, no. 4, pp. 186–189, 2000.

[17] S. S. Muir and X. Yao, "Progress in sodium borohydride as a hydrogen storage material: Development of hydrolysis catalysts and reaction systems," *Int. J. Hydrogen Energy*, vol. 36, no. 10, pp. 5983–5997, 2011.

[18] K. Mazloomi and C. Gomes, "Hydrogen as an energy carrier: Prospects and challenges," *Renew. Sustain. Energy Rev.*, vol. 16, no. 5, pp. 3024–3033, 2012.

[19] J. O. M. Bockris, "Hydrogen," *Materials (Basel).*, vol. 4, no. 12, pp. 2073–2091, 2011.

[20] J. O. M. Bockris, "The origin of ideas on a Hydrogen Economy and its solution to the decay of the environment," *Int. J. Hydrogen Energy*, vol. 27, pp. 731–740, 2002.

[21] B. M. G. Salameh, "How viable is the hydrogen economy? The case of Iceland," *Int. Assoc. Energy*

Econ., vol. 2, pp. 11–17, 2009.

[22] R. O'Hayre, S.-W. Cha, W. Colella, and F. B. Prinz, *Fuel Cells Fundamentals*, Third. Hoboken, New Jersey: John Wiley & Sons, Inc., 2016.

[23] F. Barbir, *PEM Fuel Cells: Theory and Practice*, Second. London: Elsevier Inc., 2013.

[24] U.S. Department of Energy, "Hydrogen storage | Department of Energy." [Online]. Available: https://energy.gov/eere/fuelcells/hydrogen-storage. [Accessed: 18-Oct-2017].

[25] A. Sartbaeva, V. L. Kuznetsov, S. A. Wells, and P. P. Edwards, "Hydrogen nexus in a sustainable energy future," *Energy Environ. Sci.*, vol. 1, no. 1, pp. 79–85, 2008.

[26] U. B. Demirci and P. Miele, "Sodium tetrahydroborate as energy/hydrogen carrier, its history," *Comptes Rendus Chim.*, vol. 12, no. 9, pp. 943–950, 2009.

[27] Bloomberg, "Millennium Cell Inc.: Private Company Information - Bloomberg," 2017. [Online]. Available: https://www.bloomberg.com/research/stocks/private/snapshot.asp?privcapId=527435. [Accessed: 02-Oct-2017].

[28] U. B. Demirci, O. Akdim, and P. Miele, "Ten-year efforts and a no-go recommendation for sodium borohydride for on-board automotive hydrogen storage," *Int. J. Hydrogen Energy*, vol. 34, no. 6, pp. 2638–2645, 2009.

[29] U.S. Department of Energy, "DOE Technical targets for hydrogen storage systems for portable power equipment | Department of Energy," 2012. [Online]. Available: https://energy.gov/eere/fuelcells/doe-technical-targets-hydrogen-storage-systems-portable-power-equipment. [Accessed: 18-Oct-2017].

[30] H. X. Nunes, "Hydrogen generation from catalytic hydrolysis of sodium borohydride on a mini-reactor for portable applications," Faculdade de Engenharia da Universidade do Porto, 2014.

[31] M. J. F. Ferreira, F. Coelho, C. M. Rangel, and A. M. F. R. Pinto, "Batch sodium borohydride hydrolysis systems: Effect of sudden valve opening on hydrogen generation rate," *Int. J. Hydrogen Energy*, vol. 37, no. 2, pp. 1947–1953, 2012.

[32] "Status of hydrogen storage technologies | Department of Energy," *U. S. Department of Energy*, 2008. [Online]. Available: https://energy.gov/eere/fuelcells/status-hydrogen-storage-technologies. [Accessed: 29-Sep-2017].

[33] M. J. F. Ferreira, V. R. Fernandes, L. Gales, C. M. Rangel, and A. M. F. R. Pinto, "Effects of the addition of an organic polymer on the hydrolysis of sodium tetrahydroborate in batch reactors," *Int. J. Hydrogen Energy*, vol. 35, no. 20, pp. 11456–11469, 2010.

[34] A. Pinto, D. Falcão, R. Silva, and C. Rangel, "Hydrogen generation and storage from hydrolysis of sodium borohydride in batch reactors," *Int. J. Hydrogen Energy*, vol. 31, no. 10, pp. 1341–1347, 2006.

[35] Y. Wei, W. Meng, Y. Wang, Y. Gao, K. Qi, and K. Zhang, "Fast hydrogen generation from $NaBH_4$ hydrolysis catalyzed by nanostructured Co–Ni–B catalysts," *Int. J. Hydrogen Energy*, vol. 42, no. 9, pp. 6072–6079, 2017.

[36] Y. Liang, H. Bin Dai, L. P. Ma, P. Wang, and H. M. Cheng, "Hydrogen generation from sodium borohydride solution using a ruthenium supported on graphite catalyst," *Int. J. Hydrogen Energy*, vol. 35, no. 7, pp. 3023–3028, 2010.

[37] S. Özkar and M. Zahmakiran, "Hydrogen generation from hydrolysis of sodium borohydride using Ru(0) nanoclusters as catalyst," *J. Alloys Compd.*, vol. 404–406, pp. 728–731, 2005.

[38] D. W. Zhuang, J. J. Zhang, H. Bin Dai, and P. Wang, "Hydrogen generation from hydrolysis of solid sodium borohydride promoted by a cobalt-molybdenum-boron catalyst and aluminum powder," *Int. J. Hydrogen Energy*, vol. 38, no. 25, pp. 10845–10850, 2013.

[39] P. Brack, S. E. Dann, and K. G. Upul Wijayantha, "Heterogeneous and homogenous catalysts for hydrogen generation by hydrolysis of aqueous sodium borohydride (NaBH4) solutions," *Energy Sci. Eng.*, vol. 3, no. 3, pp. 174–188, 2015.

[40] Y. Kojima, K. Suzuki, K. Fukumoto, M. Sasaki, T. Yamamoto, Y. Kawai, and H. Hayashi, "Hydrogen generation using sodium borohydride solution and metal catalyst coated on metal oxide," *Int. J. Hydrogen Energy*, vol. 27, no. 10, pp. 1029–1034, 2002.

[41] C. Wu, H. Zhang, and B. Yi, "Hydrogen generation from catalytic hydrolysis of sodium borohydride

for proton exchange membrane fuel cells," *Catal. Today*, vol. 93–95, pp. 477–483, 2004.

[42] P. Krishnan, T. Yang, W. Lee, and C. Kim, "PtRu-$LiCoO_2$—an efficient catalyst for hydrogen generation from sodium borohydride solutions," *J. Power Sources*, vol. 143, no. 1–2, pp. 17–23, 2005.

[43] Y. Bai, C. Wu, F. Wu, and B. Yi, "Carbon-supported platinum catalysts for on-site hydrogen generation from $NaBH_4$ solution," *Mater. Lett.*, vol. 60, no. 17–18, pp. 2236–2239, 2006.

[44] M. Zahmakiran and S. Özkar, "Water dispersible acetate stabilized ruthenium(0) nanoclusters as catalyst for hydrogen generation from the hydrolysis of sodium borohyride," *J. Mol. Catal. A Chem.*, vol. 258, no. 1–2, pp. 95–103, 2006.

[45] G. Guella, B. Patton, and A. Miotello, "Kinetic features of the platinum catalyzed hydrolysis of sodium borohydride from ^{11}B NMR measurements," *J. Phys. Chem. C*, vol. 111, no. 50, pp. 18744–18750, 2007.

[46] D. Xu, H. Zhang, and W. Ye, "Hydrogen generation from hydrolysis of alkaline sodium borohydride solution using Pt/C catalyst," *Catal. Commun.*, vol. 8, no. 11, pp. 1767–1771, 2007.

[47] J. S. Zhang, W. N. Delgass, T. S. Fisher, and J. P. Gore, "Kinetics of Ru-catalyzed sodium borohydride hydrolysis," *J. Power Sources*, vol. 164, no. 2, pp. 772–781, 2007.

[48] V. I. Simagina *et al.*, "Effect of the nature of the active component and support on the activity of catalysts for the hydrolysis of sodium borohydride," *Kinet. Catal.*, vol. 48, no. 1, pp. 168–175, 2007.

[49] J. Park, P. Shakkthivel, H. Kim, M. Han, J. Jang, Y. Kim, H. Kim, and Y. Shul, "Investigation of metal alloy catalyst for hydrogen release from sodium borohydride for polymer electrolyte membrane fuel cell application," *Int. J. Hydrogen Energy*, vol. 33, no. 7, pp. 1845–1852, 2008.

[50] J. C. Walter, A. Zurawski, D. Montgomery, M. Thornburg, and S. Revankar, "Sodium borohydride hydrolysis kinetics comparison for nickel, cobalt, and ruthenium boride catalysts," *J. Power Sources*, vol. 179, no. 1, pp. 335–339, 2008.

[51] Z. Liu, B. Guo, S. H. Chan, E. H. Tang, and L. Hong, "Pt and Ru dispersed on $LiCoO_2$ for hydrogen generation from sodium borohydride solutions," *J. Power Sources*, vol. 176, no. 1, pp. 306–311, 2008.

[52] C. L. Hsueh, C. Chen, J. Ku, S. Tsai, Y. Hsu, F. Tsau, and M. Jeng, "Simple and fast fabrication of polymer template-Ru composite as a catalyst for hydrogen generation from alkaline $NaBH_4$ solution," *J. Power Sources*, vol. 177, no. 2, pp. 485–492, 2008.

[53] C. W. Chen, C. Y. Chen, and Y. H. Huang, "Method of preparing Ru-immobilized polymer-supported catalyst for hydrogen generation from $NaBH_4$ solution," *Int. J. Hydrogen Energy*, vol. 34, no. 5, pp. 2164–2173, 2009.

[54] M. Zahmakiran and S. Özkar, "Zeolite-confined ruthenium(0) nanoclusters catalyst: Record catalytic activity, reusability, and lifetime in hydrogen generation from the hydrolysis of sodium borohydride," *Langmuir*, vol. 25, no. 5, pp. 2667–2678, 2009.

[55] Y. V. Larichev, O. V. Netskina, O. V. Komova, and V. I. Simagina, "Comparative XPS study of Rh/Al_2O_3 and Rh/TiO_2 as catalysts for $NaBH_4$ hydrolysis," *Int. J. Hydrogen Energy*, vol. 35, no. 13, pp. 6501–6507, 2010.

[56] Y. H. Huang, C. C. Su, S. L. Wang, and M. C. Lu, "Development of Al_2O_3 carrier-Ru composite catalyst for hydrogen generation from alkaline $NaBH_4$ hydrolysis," *Energy*, vol. 46, no. 1, pp. 242–247, 2012.

[57] C. Crisafulli, S. Scirè, R. Zito, and C. Bongiorno, "Role of the support and the Ru precursor on the performance of Ru/carbon catalysts towards H_2 production through NaBH4 hydrolysis," *Catal. Letters*, vol. 142, no. 7, pp. 882–888, 2012.

[58] Y. Li, Q. Zhang, N. Zhang, L. Zhu, J. Zheng, and B. H. Chen, "Ru-RuO_2/C as an efficient catalyst for the sodium borohydride hydrolysis to hydrogen," *Int. J. Hydrogen Energy*, vol. 38, no. 30, pp. 13360–13367, 2013.

[59] X. Li, G. Fan, and C. Zeng, "Synthesis of ruthenium nanoparticles deposited on graphene-like transition metal carbide as an effective catalyst for the hydrolysis of sodium borohydride," *Int. J. Hydrogen Energy*, vol. 39, no. 27, pp. 14927–14934, 2014.

[60] H. X. Nunes, M. J. F. Ferreira, C. M. Rangel, and A. M. F. R. Pinto, "Hydrogen generation and

storage by aqueous sodium borohydride ($NaBH_4$) hydrolysis for small portable fuel cells (H_2 – PEMFC)," *Int. J. Hydrogen Energy*, vol. 41, no. 34, pp. 15426–15432, 2016.

[61] S. Akbayrak and S. Özkar, "Inverse relation between the catalytic activity and catalyst concentration for the ruthenium(0) nanoparticles supported on xonotlite nanowire in hydrogen generation from the hydrolysis of sodium borohydride," *J. Mol. Catal. A Chem.*, vol. 424, pp. 254–260, 2016.

[62] M. Tang, G. Huang, C. Gao, X. Li, and H. Qiu, "Co nanoparticles supported 3D structure for catalytic H_2 production," *Mater. Chem. Phys.*, vol. 191, pp. 6–12, 2017.

[63] M. C. Wang, L. Z. Ouyang, J. W. Liu, H. Wang, and M. Zhu, "Hydrogen generation from sodium borohydride hydrolysis accelerated by zinc chloride without catalyst: A kinetic study," *J. Alloys Compd.*, vol. 717, pp. 48–54, 2017.

[64] M. J. F. Ferreira, C. M. Rangel, and A. M. F. R. Pinto, "Water handling challenge on hydrolysis of sodium borohydride in batch reactors," *Int. J. Hydrogen Energy*, vol. 37, no. 8, pp. 6985–6994, 2012.

[65] U. Lucia, "Overview on fuel cells," *Renew. Sustain. Energy Rev.*, vol. 30, pp. 164–169, 2014.

[66] J. Larminie and A. Dicks, *Fuel Cell Systems Explained*, 2nd ed. West Sussex, England: John Wiley & Sons, Inc., 2003.

[67] W. R. W. Daud, R. E. Rosli, E. H. Majlan, S. A. A. Hamid, R. Mohamed, and T. Husaini, "PEM fuel cell system control: A review," *Renew. Energy*, vol. 113, pp. 620–638, 2017.

[68] K. Sopian and W. R. Wan Daud, "Challenges and future developments in proton exchange membrane fuel cells," *Renew. Energy*, vol. 31, no. 5, pp. 719–727, 2006.

[69] J. I. Goldstein, D. Newbury, D. Joy, C. Lyman, P. Echlin, E. Lifshin, L. Sawyer, and J. Michael, *Scanning electron microscopy and X-ray microanalysis*, Third. New York, 2003.

[70] University of Glasgow, "University of Glasgow - Schools - School of geographical and earth sciences - research and impact - research facilities - ISAAC□: imaging spectroscopy and analysis centre - services - scanning electron microscopy." [Online]. Available: https://www.gla.ac.uk/schools/ges/researchandimpact/researchfacilities/isaac/services/scanningelectronmicroscopy/. [Accessed: 20-Nov-2017].

[71] Science Education Resource Center at Carleton College, "Scanning electron microscopy (SEM)." [Online]. Available: https://serc.carleton.edu/research_education/geochemsheets/techniques/SEM.html. [Accessed: 26-Oct-2017].

[72] How Stuff Works, "The key components of a scanning electron microscope - the key components of a scanning electron microscope | HowStuffWorks," 2009. [Online]. Available: https://science.howstuffworks.com/scanning-electron-microscope2.htm. [Accessed: 22-Nov-2017].

[73] Yale University, "SEM Principle | West campus materials characterization core," 2017. [Online]. Available: http://ywcmatsci.yale.edu/facilities/sem/sem-principle. [Accessed: 22-Nov-2017].

[74] Science Education Resource Center at Carleton College, "X-ray powder diffraction (XRD)," 2017. [Online]. Available: https://serc.carleton.edu/research_education/geochemsheets/techniques/XRD.html. [Accessed: 12-Dec-2017].

[75] M. Birkholz, "Principles of X-ray diffraction," in *Thin film analysis by X-ray scattering*, Wheinheim: Wiley-VCH Verlag GmbH & Co, 2006.

[76] University of California - Museum of Paleontology, "Understanding Science - atoms and X-rays: seeing inside a crystal," 2017. [Online]. Available: https://undsci.berkeley.edu/article/0_0_0/dna_04. [Accessed: 12-Dec-2017].

[77] M. Huang, F. Li, J. Y. Ji, Y. X. Zhang, X. L. Zhao, and X. Gao, "Facile synthesis of single-crystalline NiO nanosheet arrays on Ni foam for high-performance supercapacitors," *CrystEngComm*, vol. 16, no. 14, pp. 2878–2884, 2014.

[78] Y. Huang, S. Jiang, S.Cheng, X. Tao, Y. Zhong, G. Liao, and Z. Tang, "Enhanced cycling stability of $NiCo_2S_4$@NiO core-shell nanowire arrays for all-solid-state asymmetric supercapacitors," *Sci. Rep.*, vol. 6, no. November, p. 38620, 2016.

Appendix A Calculations performed in this work

This appendix presents the equations and defines the variables used to calculate the several parameters in all the experiments.

Firstly, it is presented the calculations for the enthalpy reaction ($\Delta H_{reaction}$) of $NaBH_4$ with water, for an *x* equal to 0.

$$NaBH_4 + 2\,H_2O \rightarrow NaBO_2 + 4H_2 \tag{A.1}$$

$$\Delta H_{reaction} = n \sum \Delta H_{products} - n \sum \Delta H_{reactants} \tag{A.2}$$

$$= \Delta H^0_{f,298K}\,(NaBO_2) + 4\,\Delta H^0_{f,298K}\,(H_2) - \Delta H^0_{f,298K}\,(NaBH_4) - 2\,\Delta H^0_{f,298K}\,(H_2O)$$

$$= (-977.0 + 4 \times 0) - (-188.6 + 2 \times (-285.8))$$

$$= 216.8\ kJ$$

Noting that $\Delta H_{product}$ and $\Delta H_{reactants}$ are the enthalpies of the products and the reactants, respectively, and $\Delta H^0_{f,298K}$ is the standard enthalpy of formation at 298 K for each compound present in the reaction.

The hydrogen generation rate, defined as *HGR*, is calculated in the next equation.

$$HGR\left(mL_{H_2} min^{-1} g^{-1}_{Cat}\right) = \frac{dP}{dt}\,\frac{V_{final}\,V_{STP}}{m_{Cat}\,RT} \times \frac{60}{1000} \tag{A.3}$$

Where dP/dt is the linear region slope, V_{STP} is the molar volume at STP conditions, respectively, *RT* is the multiplication of ideal gas constant by temperature, m_{Cat} is the catalyst mass and V_{final} is the final volume of the reactor, explained by equation (A.4).

$$V_{final}\left(cm^3\right) = V_{initial} + \left((2+x)\,\frac{m_{NaBH_4}\,MM_{H_2O}}{MM_{NaBH_4}\,\rho_{H_2O}}\right) \tag{A.4}$$

Being that *x* is the excess hydration factor, m_{NaBH_4} and MM_{NaBH_4} are the mass and molar mass of sodium borohydride, in the order mentioned, MM_{H_2O} and ρ_{H_2O} are the molar mass and density of water, respectively and $V_{initial}$ is the initial volume of the reactor, defined in the equation (A.5).

$$V_{initial}\left(cm^3\right) = V_r - \frac{m_{sol}}{\rho_{sol}} - \frac{m_{Cat}}{\rho_{Cat}} \tag{A.5}$$

V_r represents the total volume of the reactor, m_{sol}, ρ_{sol}, m_{Cat} and ρ_{Cat} the mass and densities of the solution and of the catalyst, respectively.

The yield of the reaction, η, is given by the equation:

$$\eta\ (\%) = \frac{P_{Gas_{Exp}}}{P_{Gas_{Theo}}} \times 100 \qquad (A.6)$$

where $P_{Gas_{Exp}}$ is the absolute pressure of the gas that was produced while $P_{Gas_{Theo}}$ is the absolute pressure of the gas expected in theoretical terms, assuming a 100% conversion of sodium borohydride by applying the ideal gas law to the final volume of the gas.

The gravimetric hydrogen storage capacity, *GHSC*, is calculated by the next equations.

$$GHSC\ (\text{wt}\%) = \frac{m_{H_{2_{Exp}}}}{m_{Cat} + m_{sol}} \times 100\ \text{, for alkali hydrolysis} \qquad (A.7)$$

$$\text{GHSC}\ (\text{wt}\%) = \frac{m_{H_{2_{Exp}}}}{m_{Cat} + m_{NaBH_4} + m_{H_2O}} \times 100\ \text{, for alkali-free hydrolysis} \qquad (A.8)$$

Being $m_{H_{2_{Exp}}}$ the mass of hydrogen obtained in each experience and m_{H_2O} the mass of water. It is important to note that the *GHSC* was calculated in a reactant only basis to make the comparison with literature easier.

While the *GHSC* represents a measure of the usable energy per kilogram of system mass, the volumetric hydrogen storage capacity, *VHSC*, is the same energy but per litre of system volume. Therefore, it was calculated by equations A.9 and A.10 for alkali hydrolysis.

$$VHSC\ (\text{kg m}^{-3}) = \frac{m_{H_{2_{Exp}}}}{V_{cat} + V_{sol}} \times 1000\ \text{, for alkali hydrolysis} \qquad (A.9)$$

$$VHSC\ (\text{kg m}^{-3}) = \frac{m_{H_{2_{Exp}}}}{V_{cat} + V_{NaBH_4} + V_{H_2O}} \times 1000\ \text{, for alkali-free hydrolysis} \qquad (A.10)$$

Where V_{cat}, V_{sol}, V_{NaBH_4} and V_{H_2O} are the volumes of the catalyst, of the solution, of the sodium borohydride and of water, respectively.

Appendix B Spectra obtained through Energy Dispersive X-Rays Spectroscopy

This appendix contains the spectra obtained through EDX to the several catalysts. Figure B.1 displays two spectra for different areas of the unsupported catalyst in powder form, while Figure B.2 shows a spectrum obtained to the supported catalyst ESPRU 1. Since the foams have the same support and a different concentration of catalyst, the spectrums obtained for the three catalysts presented the same elements.

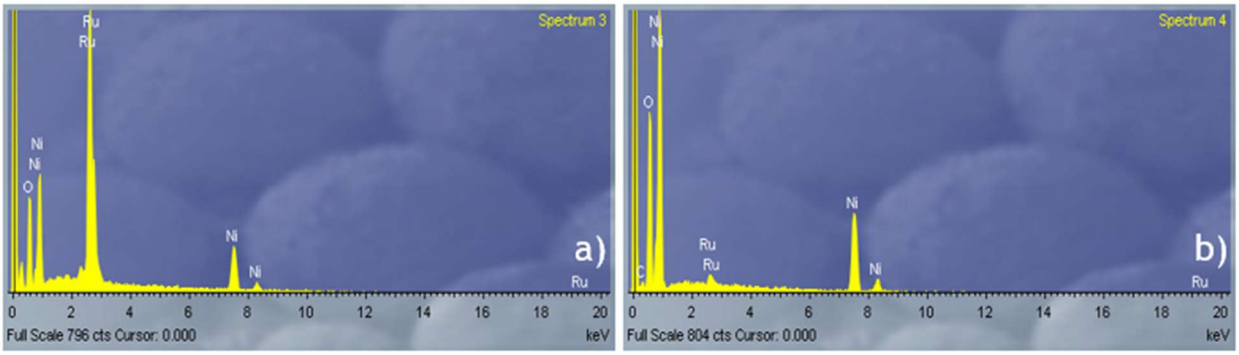

Figure B.1 - Spectra of the unsupported catalyst in the powder form never used. a) zone with a bigger amount of ruthenium; b) zone with an amount of ruthenium residual.

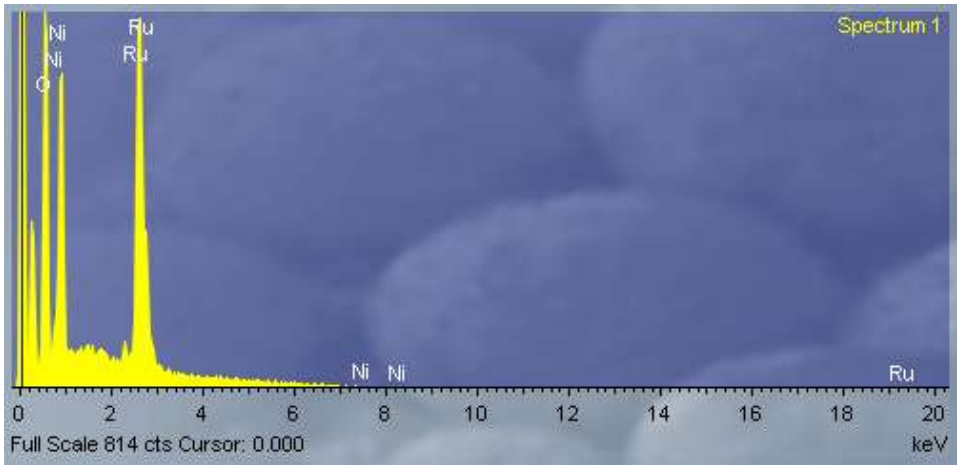

Figure B.2 – Spectrum of ESPRU 1 with 2.04 mg of catalyst.

Appendix C Images illustrating the quick degradation of the supported catalysts

An image of one of the supported catalysts after 3 and 5 reutilizations is shown in Figure C.1, where it is possible to observe the quick degradation of the catalyst, through the change of colour in the foam, which represents the loss of catalyst.

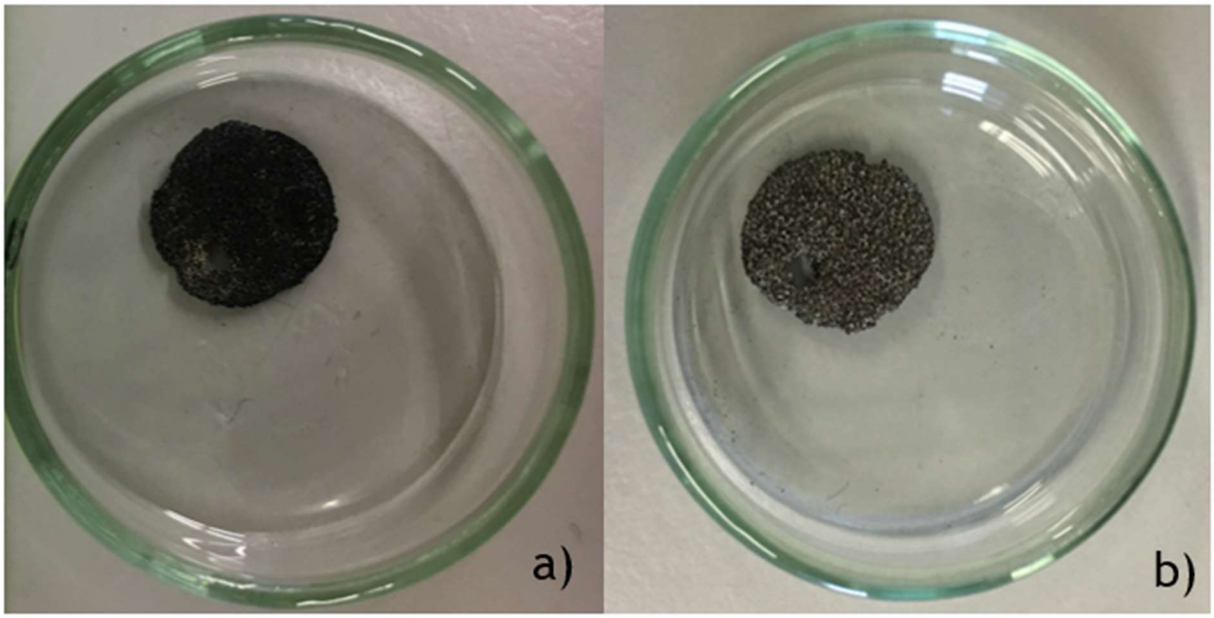

Figure C.1 – Supported catalyst ESPRU 2 (with 0.95 mg of catalyst in the support). a) After 3 reutilisations; b) After 5 reutilisations.